
# Mean Square Performance Evaluation in Frequency Domain for an Improved Adaptive Feedback Cancellation in Hearing Aids

Asutosh Kar, Ankita Anand, Jan Østergaard, Søren Holdt Jensen, M.N.S. Swamy

PII: S0165-1684(18)30363-3
DOI: https://doi.org/10.1016/j.sigpro.2018.11.003
Reference: SIGPRO 6977

To appear in: *Signal Processing*

Received date: 14 August 2017
Revised date: 8 November 2018
Accepted date: 9 November 2018

Please cite this article as: Asutosh Kar, Ankita Anand, Jan Østergaard, Søren Holdt Jensen, M.N.S. Swamy, Mean Square Performance Evaluation in Frequency Domain for an Improved Adaptive Feedback Cancellation in Hearing Aids, *Signal Processing* (2018), doi: https://doi.org/10.1016/j.sigpro.2018.11.003

**Highlights**

- The convergence, steady-state and tracking behaviour of the LP-based adaptive feedback canceller with and without probe noise depends on the adaptive algorithm employed.
- The cost of achieving an unbiased feedback cancellation using linear prediction-based adaptive feedback cancellation system with shaped probe noise is an increase in the steady-state error, in comparison with the feedback canceller without probe noise when RLS algorithm is used.
- For the NLMS algorithm, the cost of an unbiased feedback estimate is a reduction in the rate of convergence, along with an increase in the tracking error, as compared to the feedback canceller without probe noise.
- The Spectrogram-based comparison of the LP-based feedback canceller with shaped probe noise and the basic feedback canceller with probe noise for the respective loudspeaker outputs shows that the loudspeaker output of the former has less distortion and whistling problem as compared to that of the latter.
- Derived expressions provide an accurate approximation of the power transfer function, rate of convergence and steady-state error for a synthetic signal and speech signal as input, despite the assumptions made during the analysis.

# Mean Square Performance Evaluation in Frequency Domain for an Improved Adaptive Feedback Cancellation in Hearing Aids

Asutosh Kar[a,b,*], Ankita Anand[c], Jan Østergaard[b], Søren Holdt Jensen[b], M.N.S. Swamy[d]

[a] *Indian Institute of Information Technology, Design and Manufacturing, Kancheepuram, Chennai, India*
[b] *Department of Electronic Systems, Aalborg University, Denmark*
[c] *Student member, IEEE*
[d] *Department of Electrical and Computer Engineering, Concordia University, Montreal, Canada*

**Abstract**

We consider an adaptive linear prediction based feedback canceller for hearing aids that exploits two (an external and a shaped) noise signals for a bias-less adaptive estimation. In particular, the bias in the estimate of the feedback path is reduced by synthesizing the high-frequency spectrum of the reinforced signal using a shaped noise signal. Moreover, a second shaped (probe) noise signal is used to reduce the closed-loop signal correlation between the acoustic input and the loudspeaker signal at low frequencies. A power-transfer-function analysis of the system is provided, from which the effect of the system parameters and adaptive algorithms [normalized least mean square (NLMS) and recursive least square (RLS)] on the rate of convergence, the steady-state behaviour and the stability of the feedback canceller is explicitly found. The derived expressions are verified through computer simulations. It is found that, as compared to feedback canceller without probe noise, the cost of achieving an unbiased estimate of the feedback path using the feedback canceller with probe noise is a higher steady-state misadjustment for the RLS algorithm, whereas a slower convergence and

*Corresponding Author
*Email addresses:* asutoshkar@iiitdm.ac.in (Asutosh Kar), saiankitaanand@gmail.com (Ankita Anand), jo@es.aau.dk (Jan Østergaard), shj@es.aau.dk (Søren Holdt Jensen), swamy@ece.concordia.ca (M.N.S. Swamy)

a higher tracking error for the NLMS algorithm.

*Keywords:* Adaptive filters, feedback cancellation, probe noise, hearing-aid, band-limited LPC vocoder, convergence rate, power transfer function.

## 1. Introduction

Acoustic leakage takes place when an assistive listening device is vented or ill-fitted [1, 2, 3]. Consequently, the microphone of the audio system picks up a portion of the loudspeaker output signal thereby resulting in an acoustic feedback path from the system loudspeaker to the microphone. The problem of acoustic feedback degrades the performance of the audio system. In fact, the system might ultimately become unstable, causing feedback whistling and howling to occur [2, 3]. Feedback can be suppressed adaptively by using adaptive filters to identify the acoustic environment, which in turn affects the feedback path [4, 5]. Traditional approaches for controlling the feedback path problem and facilitating an unbiased solution of the feedback path can be categorized as feed-forward suppression and feedback cancellation techniques. The feed-forward suppression methods, such as gain reduction and phase modification, are based on modifying the forward signal processing path from the microphone to the loudspeaker. Feedback cancellation methods, such as feedback cancellation using adaptive filters, are based on estimating the true feedback path to generate an estimate of the original feedback signal. Among many such approaches, band-limited linear predictive coding (LPC)-based adaptive feedback cancellation (AFC) system stands out due to its effectiveness in efficiently reducing the high- frequency bias in the estimate of the original feedback path [6]. However, since a small amount of bias still persists, introduction of probe noise signal in the feedback estimation path can further reduce the bias [7]. It is essential that the probe noise signal be of a power level comparable to that of the loudspeaker signal at all frequencies and also be uncorrelated with the incoming desired signal [8]. The problem with a probe signal of a strong power level is that it is audible to the users of the assistive listening devices and thus,

undesirable. A weak probe noise signal, which is not audible to the users, reduces not only the rate of convergence of the adaptive algorithm but also the ratio of the probe noise signal and the disturbing signal [9]. A shaped probe noise signal, generated using spectral masking filters, is not annoying as it is inaudible to the users. The masking capability of the human auditory system is used by these filters so that the modified (probe-injected) loudspeaker signal, consisting of the loudspeaker input and the shaped probe signal, sounds perceptually identical to the former [10].

Adaptive feedback cancellers may employ different adaptation algorithms such as the least-mean-square (LMS), recursive least squares (RLS), normalised least-mean-square (NLMS) or variations of these algorithms [11]. From an objective point of view, the performance of a feedback canceller can be evaluated in terms of various quantities that decide the overall system behaviour. In order to determine the rate of convergence and the steady-state error of an adaptive algorithm, the feedback path is considered to be time-invariant. However, to determine the tracking error, the feedback path must be considered to be time-varying by using different variation models for the feedback path [8]. Among the many measures for evaluating the performance of a feedback canceller, the mean-square error (MSE) evaluation is the most commonly used one. The rate of convergence and the steady-state error are indicated by the decay of the MSE. The MSE evaluation method can be conveniently employed for physical measurements and simulation purposes. Another type of performance measure is the mean-square deviation (MSD) between the original feedback path and the feedback path estimate [11]. In such a performance measure, it is essential that the feedback path is already known, which is convenient for simulation purposes. In [7], the time-domain performance analysis of the adaptive feedback canceller with probe noise (discussed above) was done based on the MSE performance measure. The disadvantage of the aforementioned performance evaluation measures in time-domain is their inability to shed light upon the frequency-domain behaviour of the AFC system. The power transfer function (PTF) can be used to overcome this disadvantage and to provide fruitful knowledge about the adap-

tive system in the frequency domain [8]. The hearing impaired can hear sounds at certain frequencies and not at others. Frequency-domain analysis of the AFC design using the PTF method is more suitable than time-domain measures to study the electro-acoustic characteristics of the feedback path, the frequency-domain behavior of the feedback cancellation system and the acoustic perceptibility of the human auditory system. The PTF-based frequency-domain analysis has been done for the basic adaptive feedback canceller without probe noise in [12] and that for the AFC system with probe noise in [13]. However, in our work, we analyse the linear predictive (LP) analysis and synthesis-based AFC system with probe noise. The inclusion of LP analysis and synthesis improves the loudspeaker signal quality as compared to that in [12] by using the high-frequency portion of the synthetic replica of the reinforced signal for reducing the closed-loop signal correlations at high frequencies, and thereby reducing the bias in the adaptive estimation of the feedback path [7]. Moreover, the work done in [13] considers the use of enhancement filters for processing the error signal. However, in our work, spectral shaping filters are used to render the probe signal imperceptible in presence of the loudspeaker signal. Furthermore, since our work as well as that in [12] and [13] are based on the application of adaptive algorithms, similar measures are used for the prediction of the system behavior in all of the aforementioned works, despite analysing a different AFC framework in each case.

In this paper, we present a comparative frequency-domain performance analysis of the linear prediction-based adaptive feedback cancellers with and without probe noise in the estimation path. The approximate expressions for the PTF are derived for the linear prediction-based feedback cancellation system with as well as without the introduction of the probe noise signal in the adaptive filter path for both the RLS and NLMS adaptive algorithms. The performance of these feedback canceller schemes is discussed in terms of the convergence rate of the adaptive algorithm, system stability and their steady-state behaviour, expressions for which are derived from the aforementioned RLS algorithm-based as well as NLMS algorithm-based approximate expressions for the PTF. The

behaviour of both the feedback cancellers (with and without probe noise) is analysed and characterized for both RLS and NLMS algorithms based on the overall-system parameters and the adaptive-algorithm employed. Expressions for different adaptive-algorithm parameters are also determined for achieving desired system behaviour. The organisation of the paper is as follows. Section 2 contains a brief description of the linear prediction-based feedback cancellers with and without the probe noise signal, along with the parameters which are common to both the schemes. In Section 3, we derive detailed expression for the PTF-approximation for the RLS adaptive algorithm-based feedback cancellation scheme with probe noise in the filter estimation path; on the basis of this expression, expressions for the rate of convergence, stability constraint for the system and the steady-state behaviour of the adaptive algorithm are derived and, the influence of the overall-system parameters and the adaptive algorithm used is discussed. In Section 4, approximate expression for the PTF is derived and a discussion on the interaction between the system and its parameters is made for the NLMS adaptive algorithm-based feedback cancellation scheme with probe noise. Following the approach for the frequency-domain analysis of the feedback canceller with probe noise in Sections 3 and 4, the derivation of approximate expressions for the PTF, system-behaviour analysis and adaptive-algorithm parameters for the desired system behaviour are carried out in Section 5 for the RLS as well as NLMS adaptive algorithm-based feedback canceller without probe noise. Computer simulations are presented in Section 6 in support of the analysis and Section 7 contains the conclusions.

The following notation has been adopted throughout the paper; $[.]^T$ for the transpose of a matrix, $[.]^H$ for the Hermitian transpose of a matrix, $[.]^{-1}$ for the inverse of a matrix, $[.]^*$ for complex conjugation, $E[.]$ for the expectation operation, $n$ for discrete-time index, $k$ for discrete-time delay operator such that $k^{-1}m(n) = m(n-1)$ , $\omega$ for frequency, bold-faced lower-case letters for column vectors and bold-faced upper-case letters for matrices. A discrete-time filter of length $L$ is represented as a polynomial $F(k)$ in terms of $k^{-1}$ as $F(k) = f_0 + f_1k^{-1} + ... + f_{L-1}k^{-L+1}$ or by its coefficient vector $\mathbf{f} = [f_0, f_1, ..., f_{L-1}]^T$.

The signal $m(n)$ is filtered by $F(k)$ as $F(k)m(n) = \mathbf{f}^T(n)\,\mathbf{m}(n)$ , with $\mathbf{m}(n) = [m(n), m(n-1), ..., m(n-L+1)]^T$. $F(\omega, n)$ denotes the frequency response of $F(k)$ .

## 2. System Description

The block diagram of the linear prediction-based feedback cancellation system, with a shaped probe noise signal introduced in the filter estimation path, is shown in Fig. 1. A similar AFC system without probe noise, introduced in [6], is shown in Fig. 2. In this section, we consider the linear prediction-based feedback cancellers, with and without the probe-noise signal, on the basis of some welldefined system parameters. We formulate the PTF to facilitate further study of the frequency-domain behaviour of the feedback cancellers shown in Figs. 1 and 2, respectively. The fundamental idea of the linear prediction-based approach is based on the production of a synthetic copy of the forward processed signal such that it is identical, but uncorrelated with the desired sound signal [6]. The feedback signal $f_b(n)$ is formed when the loudspeaker signal is passed though the acoustic environment represented by $F(k)$. We consider $F(k)$ as an FIR filter of length $L_f$ and coefficient vector $\mathbf{f} = [f_0, f_1, ..., f_{L-1}]^T$. The adaptive filter $\hat{F}(k)$ is also considered as an FIR filter of length $L_{\hat{f}}$ and the coefficient vector $\hat{\mathbf{f}} = [\hat{f}_0, \hat{f}_1, ..., \hat{f}_{L_{\hat{f}}-1}]^T$.

The time-varying behaviour of $F(k)$ can be represented using the Random-Walk model [14, 15] as

$$F(\omega, n) = F(\omega, n-1) + \breve{F}(\omega, n), \tag{1}$$

where $F(\omega, n)$ is the frequency response of the feedback path $F(k)$ and $\breve{F}(\omega, n)$ is considered as the frequency response of the variation vector of the feedback path. We consider the variation vector of the feedback path to be a Gaussian random process of zero mean such that $\breve{F}(\omega, n)$ is a complex quantity [8, 14]. The power spectral density of $\breve{F}(\omega, n)$ is given as

$$S_{\breve{f}}(\omega) = E\left[\breve{F}(\omega, n)\,\breve{F}^*(\omega, n)\right]. \tag{2}$$

To get a preliminary expression of the PTF, we start with the time-domain representation of the system parameters. The feedback path variation vector is

$$\breve{\mathbf{f}}\left(n\right)=\mathbf{f}\left(n\right)-\mathbf{f}\left(n-1\right), \tag{3}$$

where $\breve{\mathbf{f}}=[\breve{f}_0,\breve{f}_1,...,\breve{f}_{L_f-1}]^T$. Similarly, we can express the feedback path estimation-error vector $\tilde{\mathbf{f}}=[\tilde{f}_0,\tilde{f}_1,...,\tilde{f}_{L_f-1}]^T$ as the difference between the coefficient vector of the adaptive estimator and the original feedback path as

$$\tilde{\mathbf{f}}\left(n\right)=\hat{\mathbf{f}}\left(n\right)-\mathbf{f}\left(n\right). \tag{4}$$

Considering Figs. 1 and 2, the microphone signal

$$y\left(n\right)=x\left(n\right)+f_{\mathrm{b}}\left(n\right). \tag{5}$$

The error signal

$$e\left(n\right)=y\left(n\right)-v\left(n\right), \tag{6}$$

where $v\left(n\right)$ is the output of the adaptive filter. The loudspeaker signal

$$q\left(n\right)=u_{\mathrm{lp}}\left(n\right)+u_{\mathrm{syn\_hp}}\left(n\right), \tag{7}$$

where the signal vector $\mathbf{q}=\left[q\left(n\right),q\left(n-1\right),...,q\left(n-L_{\hat{f}}+1\right)\right]^T$, and $u_{\mathrm{lp}}\left(n\right)$ is the low-frequency component of the reinforced forward path signal $u\left(n\right)$ and $u_{\mathrm{syn\_hp}}\left(n\right)$ is the high-frequency component of the synthetic version of $u\left(n\right)$ with vector definitions $\mathbf{u}_{\mathrm{lp}}\left(n\right)=\left[u_{\mathrm{lp}}\left(n\right),u_{\mathrm{lp}}\left(n-1\right),...,u_{\mathrm{lp}}\left(n-L_{\hat{\mathrm{f}}}+1\right)\right]^T$ and $\mathbf{u}_{\mathrm{syn\_hp}}\left(n\right)=\left[u_{\mathrm{syn\_hp}}\left(n\right),u_{\mathrm{syn\_hp}}\left(n-1\right),...,u_{\mathrm{syn\_hp}}\left(n-L_{\hat{\mathrm{f}}}+1\right)\right]^T$ respectively. The low-pass filter $L_{\mathrm{P}}\left(k\right)$ is designed to allow only the frequency spectrum of $u\left(n\right)$ below 2 kHz to pass through, the high-pass filter $H_{\mathrm{P}}\left(k\right)$ is designed to allow only the 2 kHz spectrum to pass through, and $\hat{H}\left(k\right)$ is the estimated $P^{\mathrm{th}}$ order all-pole signal model which is used to obtain a synthetic replica of $u\left(n\right)$ and is a part of the LP analysis and synthesis block in Figs. 1 and 2 [6]. The gain $G\left(k\right)$ of the hearing aid provides reinforcement to the error signal $e\left(n\right)$, and can be expressed as

$$G\left(k\right)=k^{-d_{\mathrm{g}}}\bar{G}\left(k\right),\ d_{\mathrm{g}}\geq 1, \tag{8}$$

where $d_{\mathrm{g}}$ is the time-delay and $\bar{G}(k)$ is the transfer function which provides a frequency-specific reinforcement to the error signal to reduce the listening effort [6].

In Fig. 1, the shaped probe noise signal $r_{\mathrm{s}}(n)$ is generated by passing a Gaussian white-noise sequence $r(n)$ of zero mean and unit variance through a spectral shaping filter $A(k)$ with coefficient vector $\mathbf{a}(n) = [a_0, a_1, ..., a_{L_{\hat{s}}-1}]^T$ as

$$r_{\mathrm{s}}(n) = A(k)\, r(n). \tag{9}$$

Considering Fig. 1, the probe-injected loudspeaker output can be expressed in vector form as

$$\mathbf{q}_{\mathrm{r}}(n) = \mathbf{q}(n) + \mathbf{r}_{\mathrm{s}}(n), \tag{10}$$

where $\mathbf{q}_{\mathrm{r}} = \left[q_{\mathrm{r}}(n), q_{\mathrm{r}}(n-1), ..., q_{\mathrm{r}}\left(n - L_{\hat{f}} + 1\right)\right]^T$, $\mathbf{q} = \left[q(n), q(n-1), ..., q\left(n - L_{\hat{f}} + 1\right)\right]^T$ and $\mathbf{r}_{\mathrm{s}} = \left[r_{\mathrm{s}}(n), r_{\mathrm{s}}(n-1), ..., r_{\mathrm{s}}\left(n - L_{\hat{f}} + 1\right)\right]^T$.

The frequency-domain expression of the MSD is referred to as the PTF [8]. In this work, the frequency-domain expression for the MSD between the original feedback path and the feedback path estimate, i.e. $E\left[\left\|\mathbf{f}(n) - \hat{\mathbf{f}}(n)\right\|^2\right]$, is the PTF which can conveniently describe the behaviour of an adaptive feedback canceller. The open-loop transfer function of the closed-loop AFC system in Fig. 1 and Fig. 2, for a specific frequency $\omega$ and time-instant $n$, is given as

$$O(\omega, n) = G(\omega, n)\, L_{\mathrm{p}}(\omega, n)\left(F(\omega, n) - \hat{F}(\omega, n)\right). \tag{11}$$

If we consider the closed-loop AFC system in Figs. 1 and 2 to be linear and time-invariant, then as per the Nyquist stability criterion, they will be unstable when [16]

$$\begin{aligned} &\left|G(\omega, n)\, L_{\mathrm{p}}(\omega, n)\left(F(\omega, n) - \hat{F}(\omega, n)\right)\right| \geq 1 \\ &\angle G(\omega, n)\, L_{\mathrm{p}}(\omega, n)\left(F(\omega, n) - \hat{F}(\omega, n)\right) = j2\pi, \end{aligned} \tag{12}$$

where $j$ is an integer. Generally, the feedback path $F(k)$ is not known apriori and thus it is not possible to calculate the open-loop transfer function $O(\omega, n)$.

However, we can express the expected value of the magnitude-square of $O(\omega, n)$ as

$$E\left[|O(\omega, n)|^2\right] = |G(\omega, n)\, L_{\mathrm{p}}(\omega, n)|^2 \zeta(\omega, n), \tag{13}$$

where $\zeta(\omega, n)$ is the expected value of the magnitude-squared transfer function between points A and B[1] in Figs. 1 and 2; this transfer function is also called as the PTF. It can be written in terms of the MSE in frequency domain for a feedback cancellation framework as [14]

$$\zeta(\omega, n) = E\left[\left|\hat{F}(\omega, n) - F(\omega, n)\right|^2\right]. \tag{14}$$

From the above equation, it can be observed that for an ideal feedback cancellation system where $\hat{F}(\omega, n) = F(\omega, n)$, the value of the PTF will be equal to zero at all frequencies. However, in practical applications, $\zeta(\omega, n)$ is random in nature as the original feedback path is unknown and changes randomly [12]. Substituting the frequency-domain version of (4) into (14), an expression for the PTF can be expressed as [14]

$$\zeta(\omega, n) = E\left[\tilde{F}(\omega, n)\, \tilde{F}^*(\omega, n)\right], \tag{15}$$

where $\tilde{F}(\omega, n)$ is the frequency response of the feedback path estimation-error signal $\tilde{f}(n)$. The reinforcement filter $G(k)$ and thereby, its frequency response $G(\omega, n)$, is already known. Consequently, the expectation of the magnitude-squared $O(\omega, n)$ in (13) can be determined. However, the problem is that $O(\omega, n)$ is considered to be random in nature and is unknown a priori due to $\tilde{F}(\omega, n)$ being unknown. As a result, the PTF cannot be computed directly. Hence, if we can obtain an approximation of $\tilde{F}(\omega, n)$, an expression for approximate-PTF $\hat{\zeta}(\omega, n)$ can be conveniently obtained using (15). The importance of the expression for approximate-PTF $\hat{\zeta}(\omega, n)$ is that it allows us

[1] All derivations in this work are done after omitting the reinforcement filter $G(k)$, i.e., on an open-loop setup. However, the simulations were performed for a closed-loop AFC system of a hearing aid, with a delay inserted in the forward path [12]. It was found that the derivations were applicable for the closed-loop system and results were verified.

to analyse and characterize the behaviour of the AFC system using statistical characteristics of the signals, order of the adaptive filter, adaptive algorithm used and the assumptions made for the variations in the feedback path, when the feedback path is not known apriori [8, 17]. The following assumptions are made in this paper for further analysis:

i The shaped probe noise signal $r_s(n)$ and the unshaped probe noise signal $r(n)$ are assumed to be uncorrelated with the desired signal $x(n)$ and with loudspeaker signal $q(n)$.

ii A sufficiently large filter length $L_{\hat{f}}$ of the adaptive-estimation filter models the unknown feedback path to avoid undermodelling and the length $L_{\hat{f}}$ of the adaptive filter is assumed to be identical to the length $L_f$ of the feedback path [12, 18].

iii The length $L_{\mathrm{a}}$ of the shaping filter $A(k)$ is assumed to be less than the length $L_{\hat{f}}$ of the adaptive estimator, i.e. $L_{\mathrm{a}} < L_{\hat{f}}$ in the system of Fig. 1.

iv The incoming desired acoustic signal $x(n)$ is considered to be a stationary random signal of zero mean. The input auto-correlation $r_x(m)$ expressed as $r_x(m) = E[x(n)\,x(n-m)]$ such that $r_x(m) = 0 \forall |m| > m_0$, where $m_0$ is a finite integer.

v With reference to the expression in (3) for the feedback path variation vector $\breve{\mathbf{f}}(n)$, the variations in the feedback path are independent of $x(n)$, $\mathbf{q}(n)$, $\mathbf{r}_{\mathrm{s}}(n)$ and $\tilde{\mathbf{f}}(n)$ [8].

## 3. Frequency-domain analysis for RLS algorithm

In this section, we derive an expression for the PTF-approximate $\hat{\zeta}(\omega, n)$ for the RLS adaptive algorithm for the feedback cancellation system shown in Fig. 1. The RLS adaptive algorithm gives faster convergence, albeit at an additional cost of computational complexity, as compared to the NLMS algorithm[11]. Further, we use the derived expression for $\hat{\zeta}(\omega, n)$ for analysing the effect of the

system parameters and the RLS algorithm parameters on the system behaviour. We also find the expression to allow for the choice of a forgetting-factor value that facilitates a required system property.

### *3.1. Approximate expression for PTF*

**Theorem 1.** *Consider the linear prediction-based adaptive feedback canceller with shaped probe noise in Fig. 1. Let the adaptive filter $\hat{F}(k)$ be updated using the RLS algorithm, and suppose that assumptions (i)-(v) hold. Then, the PTF of (15) can be written as*

$$\hat{\zeta}(\omega, n) = (2\lambda - 1)\,\hat{\zeta}(\omega, n-1) + L_f \frac{(1-\lambda)^2}{|A(\omega)|^2 S_r(\omega)} S_x(\omega) + S_{\widetilde{f}}(\omega), \qquad (16)$$

*where $\lambda$ is the forgetting factor such that $0 < \lambda < 1$, $L_f$ is the length of the feedback path, $A(\omega)$ is the frequency response of shaping filter $A(k)$, $S_r(\omega)$ is the PSD of unshaped probe noise $r(n)$, $S_x(\omega)$ is the PSD of the incoming acoustic signal $x(n)$ and $S_{\widetilde{f}}(\omega)$ is the variance of the feedback path.*

*Proof.* The detailed derivation of the approximate expression for the PTF of the linear prediction-based AFC system with shaped probe noise is presented in a step-wise manner in Appendix A. □

We will now use the PTF expression in (16) to derive and predict the system behaviour in terms of the rate of convergence, steady-state error and tracking error.

### *3.2. Prediction of system behaviour*

The convergence rate (CR) can be determined as the decay-rate of the MSD between the original and the estimated feedback path. In frequency domain, convergence rate can be defined as the decay of the PTF $\zeta(\omega, n)$ as the iterations progress and can be written as

$$\mathrm{CR} = \lim_{n\to\infty} \frac{d}{dn}\,\zeta(\omega, n). \qquad (17)$$

It will be seen later in this work that for the RLS algorithm, CR is independent of $\omega$, whereas it is a function of $\omega$ for the NLMS algorithm. Hence, the convergence

rate is simply mentioned as CR in (17). The steady-state error (SSE) is the final MSD value between the true and the estimated feedback path, corresponding to a stationary feedback path, and can be written as

$$\mathrm{SSE}\left(\omega\right) = \lim_{n\to\infty} E\left[\left|\hat{F}\left(\omega,n\right) - F\left(\omega,n\right)\right|^2\right],\ S_{\breve{f}}\left(\omega\right) = 0. \tag{18}$$

The tracking error (TE) is the misadjustment in tracking the non-stationary feedback path and can be expressed as

$$\mathrm{TE}\left(\omega,n\right) = E\left[\left|\hat{F}\left(\omega,n\right) - F\left(\omega,n\right)\right|^2\right],\ S_{\breve{f}}\left(\omega\right) \neq 0. \tag{19}$$

Lemma 1 derives the expressions for the convergence rate defined in (17), the steady-state error in (18) and tracking error in (19) for the linear prediction-based feedback canceller with shaped probe noise in Fig. 1 to analyse the system behaviour when RLS adaptive algorithm is used.

**Lemma 1.** *For the AFC system in Fig. 1 and under the assumptions stated in Section 2, the following holds*

*i System convergence (CR) in (17) slows down with increasing $\lambda$.*

*ii SSE in (18) increases with increasing $L_f$ and $S_x\left(\omega\right)$, and with decreasing $\lambda$ and $S_p\left(\omega\right)$*

*iii TE in (19) increases with increasing $\lambda$ for $S_{\breve{f}}\left(\omega\right) > 0$*

*Proof.* The proof of Lemma 1 is presented in detail in Appendix C. □

We will use the expression obtained in (C.9) in the proof of Lemma 1 to obtain the value of forgetting factor of the RLS algorithm for achieving a desired system behaviour in Corollary 1.

**Corollary 1.** *For the system in Fig. 1 and under assumptions (i)-(v), the selection of the forgetting factor value, for achieving a required rate of convergence of the RLS adaptive algorithm, can be carried out according to*

$$\lambda = \frac{1 + 10^{\frac{\mathrm{CR}}{10}}}{2}, \tag{20}$$

*the convergence rate CR being in dB per iterative instant n. The selection of the forgetting factor for obtaining the desired steady-state error* $\hat{\zeta}(\omega,\infty)$ *can be done according to*

$$\lambda = 1 - \frac{2\,S_p(\omega)\,\hat{\zeta}(\omega,\infty)}{L_f\;S_x(\omega)}. \tag{21}$$

*Proof.* The proof of Corollary 1 is presented in detail in Appendix C. □

## 4. Frequency-domain analysis for NLMS algorithm

In this section, following the treatment in the proof of Theorem 1, we derive an approximate expression for the PTF for the NLMS adaptive algorithm for the feedback cancellation system shown in Fig. 1. Moreover, we use this derived expression for analysing the effect of the system parameters and the NLMS algorithm parameters on the system behaviour. We also find the expression that allows the choice of a step size value, which facilitates a required system characteristic.

### *4.1. Approximate expression for the PTF*

**Corollary 2.** *For the feedback canceller with shaped probe noise in Fig. 1, where* $\hat{F}(k)$ *is updated using the NLMS algorithm and under assumptions (i)-(v), the PTF of (15) can be written as*

$$\begin{aligned}\hat{\zeta}(\omega,n) = &\left(1 - 2\frac{\tilde{\mu}(n)}{\delta + L_f\,\sigma_p^2}\,S_p(\omega)\right)\hat{\zeta}(\omega,n-1)\\ &+ L_f\frac{\tilde{\mu}^2(n)}{\left(\delta + L_f\sigma_p^2\right)^2}\,S_p(\omega)\,S_x(\omega) + S_{\breve{f}}(\omega),\end{aligned} \tag{22}$$

*where* $S_p(\omega)$ *is the PSD of shaped probe noise* $r_s(n)$*,* $\tilde{\mu}(n)$ *is the normalized step size of the adaptive algorithm,* $\delta$ *is a small positive real number and* $\sigma_p^2$ *is the variance of* $r_s(n)$*.*

*Proof.* The detailed derivation of the approximate expression for the PTF of the linear prediction-based AFC system with shaped probe noise is presented in a step-wise manner in Appendix D, with reference to the NLMS adaptive algorithm. □

*4.2. Prediction of system behaviour*

Lemma 2 derives the expressions for the convergence rate defined in (17), the steady-state error in (18) and the tracking error in (19) for the linear AFC system in Fig. 1 to analyse the system behaviour when NLMS adaptive algorithm is used.

**Lemma 2.** *For the AFC system in Fig. 1 and under assumptions (i)-(v), the following holds*

*i System CR in (17) increases with increasing* $\tilde{\mu}(n)$

*ii SSE in (18) increases with increasing values of* $L_f$ *and* $\tilde{\mu}(n)$*, and with decreasing value of* $S_x(\omega)$

*iii TE in (19) increases with increasing* $L_f$*, as well as with a decreasing ratio of* $S_p(\omega) / \left(\delta + L_f \sigma_p^2\right)$

*Proof.* The proof of Lemma 2 is presented in detail in Appendix D. □

The expression in (D.11) can now be used to derive an expression for obtaining the value of step size parameter for a required system behaviour characteristic.

**Corollary 3.** *For the AFC system in Fig. 1 and under assumptions (i)-(v), selection of the normalized step-size parameter for the NLMS algorithm, to achieve a required given rate of convergence, can be carried out according to*

$$\tilde{\mu}(n) = \left(\delta + L_f \sigma_p^2\right) \frac{1 - 10^{\frac{\mathrm{CR}}{10}}}{2 S_p(\omega)}, \tag{23}$$

*CR being in dB per iterative instant* $n$*, and the selection of the normalized step-size parameter for obtaining the desired steady-state error* $\hat{\zeta}(\omega, \infty)$*, corresponding to a time-invariant feedback path, can be done according to*

$$\tilde{\mu}(n) = \frac{2\left(\delta + L_f \sigma_p^2\right) \hat{\zeta}(\omega, \infty)}{L_f S_x(\omega)}. \tag{24}$$

*Proof.* The proof of Corollary 3 is presented in detail in Appendix D. □

**Remark 1.** *In a feedback cancellation design with probe noise, it is desired that the probe noise $r(n)$ be inaudible to the listeners in presence of the loudspeaker signal $q(n)$ such that $q_r(n)$ is perceived as $q(n)$. To achieve this, a shaped probe noise $r_s(n)$, instead of $r(n)$, is added to $q(n)$ to facilitate an unbiased estimation. The shaped probe noise exploits the masking capabilities of the auditory system in humans and $S_p(\omega)$ is chosen to be approximately 15-25 dB below $S_q(\omega)$ [8], [19].*

**Remark 2.** *Here, we present the delay condition for achieving an unbiased solution for the feedback path. For this, we consider Fig. 1 when $r_s(n)$ is used in the estimation path of the AFC system. A shaped probe signal reduces the decorrelation effect, which is required to reduce the bias in the estimate of the feedback path [18]. The optimal solution for the feedback path is biased, even when $r_s(n)$ is a white-noise signal [7, 20]. This shows that the shaping filter introduces a bias in the feedback path estimate, which can be prevented by introducing a sufficiently large delay in the forward path [18]. Let us assume that $r_s(n)$ has a finite correlation function as*

$$R_p(m) = 0 \,\forall\, |m| > m_0, \tag{25}$$

*where $m_0$ is a finite integer. As presented in [7, 21], an unbiased optimal solution for the feedback path is possible when*

$$d_g \geq L_f + m_0. \tag{26}$$

*From (8), it can be seen that the forward path $G(k)$ consists of a delay $d_g$ along with the actual reinforcement filter $\bar{G}(k)$ of length $L_{\bar{g}}$. In order to prevent $\bar{G}(k)$ from contributing to the bias in the feedback path estimate, the delay $d_g$ introduced in the forward path should be such that*

$$d_g \geq L_f + m_0 + L_{\bar{g}}. \tag{27}$$

*The above equation presents a general delay condition for achieving a bias-free estimate of the feedback path, when a shaped probe noise signal is introduced in the filter estimation path of the linear prediction-based AFC system.*

Table 1 summarizes the effect of the overall-system parameters on the behaviour of the feedback cancellation design in Fig. 1, based on the choice of the adaptive algorithm (NLMS or RLS).

## 5. Frequency-domain analysis for the feedback canceller without probe noise

**Corollary 4.** *For the linear prediction-based adaptive feedback canceller without probe noise in Fig. 2, in which $\hat{F}(k)$ is updated using the RLS algorithm and supposing that assumptions (ii)-(v) hold, the PTF of (15) can be written as*

$$\hat{\zeta}(\omega, n) = (2\lambda - 1)\,\hat{\zeta}(\omega, n-1) + L_f \frac{(1-\lambda)^2}{S_q(\omega)} S_x(\omega) + S_{\breve{f}}(\omega), \qquad (28)$$

*where $S_q(\omega)$ is the PSD of the loudspeaker signal $q(n)$.*

*Proof.* The approximate expression for the PTF of the linear prediction-based AFC system in Fig. 2 can be derived following the proof of Theorem 1. For detailed derivation, see Appendix E. □

Lemma 3 derives the expressions for the convergence rate in (17), the steady-state error in (18) and the tracking error in (19) for the feedback canceller without probe noise (see Fig. 2) to analyse the system behaviour when RLS adaptive algorithm is used.

**Lemma 3.** *For the system in Fig. 2, and under assumptions (ii)-(v), the following holds*

*i System CR in (17) decreases with increasing $\lambda$*

*ii SSE in (18) increases with increasing $L_f$ and $S_p(\omega)$, and with decreasing $\lambda$ and $S_p(\omega)$*

*iii TE in (19) decreases with increasing $\lambda$ for $S_{\breve{f}}(\omega) > 0$*

*Proof.* The proof for the above follows Lemma 1 and is presented in Appendix E. □

**Corollary 5.** *The selection of the forgetting factor value to achieve a required given rate of convergence can be done as (20) where the convergence rate is in dB per iterative instant $n$, and the selection for forgetting factor value for obtaining desired steady-state error $\hat{\zeta}(\omega,\infty)$ can be done according to*

$$\lambda = 1 - \frac{2\,S_q(\omega)\,\hat{\zeta}(\omega,\infty)}{L_f S_x(\omega)}. \tag{29}$$

*Proof.* The proof for the above follows that of Corollary 1 and is presented in Appendix E. □

**Corollary 6.** *For the feedback canceller in Fig. 2 using the NLMS adaptive algorithm and under assumptions (ii)-(v), the PTF of (15) can be written as*

$$\hat{\zeta}(\omega,n) = \left(1 - 2\frac{\tilde{\mu}(n)}{\delta + L_f\sigma_q^2} S_q(\omega)\right)\hat{\zeta}(\omega,n-1) + L_f \frac{\tilde{\mu}^2(n)}{\left(\delta + L_f\sigma_q^2\right)^2} S_q(\omega)\,S_x(\omega) + S_{\widetilde{f}}(\omega). \tag{30}$$

*Proof.* The proof for the above follows that of Corollary 1 and is presented in Appendix F. □

Lemma 4 derives the expressions for the convergence rate in (17), the steady-state error in (18) and the tracking error in (19) for the linear prediction-based feedback canceller without probe noise (see Fig. 2) to analyse the system behaviour when NLMS adaptive algorithm is used.

**Lemma 4.** *For the AFC system in Fig 2, and under assumptions (ii)-(v), the following hold*

*i System CR in (17) decreases with increasing $L_f$*

*ii SSE in (18) increases with increasing $L_f$, $\tilde{\mu}(n)$ and $S_x(\omega)$, and with decreasing $\sigma_q^2$*

*iii TE in (19) increases with increasing $L_f$ and with decreasing ratio of $S_q(\omega)$ / $\left(\delta + L_f\,\sigma_q^2\right)$*

*Proof.* The proof for the above follows that of Lemma 2 and is presented in Appendix F. □

**Corollary 7.** *For the system in Fig. 2 and under assumptions (ii)-(v), the selection of the normalized step-size parameter for the NLMS algorithm, to achieve a required given rate of convergence, can be done according to*

$$\tilde{\mu}\left(n\right) = \left(\delta + L_f \sigma_q^2\right) \frac{1 - 10^{\frac{\mathrm{CR}}{10}}}{2\, S_q\left(\omega\right)}, \tag{31}$$

*where the convergence rate is in dB per iterative instant $n$, and the selection of the normalized step-size parameter for obtaining the desired steady-state error $\hat{\zeta}\left(\omega, \infty\right)$ can done according to*

$$\tilde{\mu}\left(n\right) = \frac{2\left(\delta + L_f\, \sigma_q^2\right) \hat{\zeta}\left(\omega, \infty\right)}{L_f\, S_x\left(\omega\right)}. \tag{32}$$

*Proof.* The proof for the above follows that of Corollary 3 and is presented in Appendix F. □

**Remark 3.** *From Lemmas 1 and 3, it can be concluded that when RLS adaptive algorithm is used, the steady-state error in the feedback canceller with shaped probe noise is increased by a factor of $S_q\left(\omega\right)/S_p\left(\omega\right)$, as compared to that for the feedback canceller without probe noise.*

**Remark 4.** *From Lemmas 2 and 4, it can be concluded that using NLMS algorithm with the same value of step size and for the same values of $\sigma_q^2$ and $\sigma_p^2$, the values of steady-state error obtained are identical but the rate of convergence of the feedback cancellation system with shaped probe noise is decreased by a factor of $S_q\left(\omega\right)/S_p\left(\omega\right)$, as compared to that for the feedback cancellation system without probe noise. Similarly, the tracking error of the feedback canceller with shaped probe noise is increased by a factor of $S_q\left(\omega\right)/S_p\left(\omega\right)$ as compared to that for the feedback canceller without probe noise.*

A brief description of the relation between the overall-system parameters and the behaviour of the feedback canceller in Fig. 2 is presented in Table 2.

## 6. Simulation and Results

In this section, we consider the behaviour of the linear prediction-based adaptive feedback canceller with and without a probe noise signal in the feedback estimation path. The goal of the simulations presented in this section is to verify the derived expressions for the PTF, rate of convergence and steady-state error and compare the performance of the feedback cancellers in Figs. 1 and 2. The simulations have been performed on MATLAB using a sampling frequency of 16 kHz.

The original feedback path is known during the simulation and is considered to be an FIR filter of order 50. Fig. 3 shows the magnitude response of the original feedback path obtained using a behind-the-ear hearing aid. A higher magnitude of the feedback path from 2 to 7 kHz shows that the feedback oscillations are more likely to occur at higher frequencies. The feedback estimation filter is also an FIR filter of order 50. The forward path consists of a simple hearing aid gain $|\bar{G}| = 5$ and a delay $d_{\mathrm{g}} = 57$. The frequency response of the complementary filter pair of the high-pass filter $H_{\mathrm{p}}(k)$ and the low-pass filter $H_{\mathrm{p}}(k)$ of order 40 and a cut-off frequency of 2 kHz is shown in Fig. 4. The Band-limited linear prediction vocoder reduces the correlation between $x(n)$ and $q(n)$ and facilitates an unbiased PTF expression. Thus, there is no need to use additional shaping filters for them as is done in [8]. The unshaped probe noise signal is considered as a zero-mean and unit-variance white-Gaussian-noise signal. The shaping filter is also an FIR filter of order 1 [8, 18, 21] and has a coefficient vector $\mathbf{a}(n) = [1,\ -0.3]^T$. The value of the forgetting factor is chosen as 0.99 (see footnote 2).

### *6.1. Synthetic signal as input*

The feedback path remains fixed for the first half of the simulation. According to the random-walk model represented as $f(i,n) = f(i,0) + \sum_{m=10^4}^{n} \varepsilon_f(m)$, where $f(i,n)$ is the $i^{\mathrm{th}}$ tap of the original feedback path impulse response at a time instant $n$ and $\varepsilon_f(m)$ is the $m^{\mathrm{th}}$ sample of the realization of a Gaussian

random sequence with mean $\mu_f = 0$ and variance $\sigma_f^2 = 0.014$, is introduced in the subsequent half of the simulation experiment. A stable signal-model estimate of order 20 can be obtained using the LP analysis window length of 20 ms. The input signal is a synthetic signal produced by passing a new realization of a Gaussian random sequence through a shaping filter with an impulse response $[1, -0.5]^T$, for each simulation run. We have chosen the level of the probe noise signal to be 1.414 times the level of the loudspeaker signal for the ease of simulation. We have computed the PTF approximate expression by taking an average of the values over 100 simulation runs of 2x$10^4$ iterations each, at example frequency $\omega = \frac{2\pi\, m}{L_f}$, where $m = 7, 12$.

Fig. 5(a) shows the simulation of the feedback canceller with shaped probe noise using (C.2) and (C.9), and Fig. 5(b) shows the simulation of the feedback canceller without probe noise using (C.2) and (E.11) for the frequency bin $m = 7$. Fig. 6(a) shows the simulation of feedback cancellation design with shaped probe noise using (C.2) and (C.9), and Fig. 6(b) shows the simulation of feedback cancellation design without probe noise using (C.2) and (E.11) for the frequency bin $m = 12$. Comparing Fig. 5(a) with Fig. 5(b), it can be seen that the rate of convergence for the adaptive feedback canceller without probe noise and the adaptive feedback canceller with shaped probe noise remains constant for the same value of $\lambda$ at the example frequency bin $m = 7$. Similarly, for the same value of $\lambda$, it can be seen from Fig. 6(a) and Fig. 6(b) that the convergence rate for both the aforementioned systems remains constant at the example frequency bin $m = 12$. This is because the convergence rate for the RLS algorithm depends only on $\lambda$ and not on the frequency or any other signal property. In this work, since $S_q(\omega) = 2\, S_{\mathrm{p}}(\omega)$, the steady-state error in Fig. 5(a) is increased by a factor of 2 as compared to that in Fig. 5(b). As a result, the sum of the steady-state and the tracking errors has also increased in Fig. 5(a) as compared to that in Fig. 5(b). Similarly, the steady-state error and the sum of the steady-state and the tracking errors are increased in Fig. 6(a) as compared to that in Fig. 6(b).

Fig. 7 shows the simulation of the AFC system with shaped probe noise using

(20), and a forgetting-factor value of 0.9983 for a desired value of the steady-state error. It can be observed from Figs. 5, 6 and 7 that the simulations verify the derived expressions.

### *6.2. Speech signal as input*

To demonstrate the application of the proposed algorithm in practical scenarios, a female-spoken speech segment of 5 seconds was chosen as an input to the hearing-aid system shown in Fig. 1 and to the basic adaptive feedback canceller presented in [8, 18]. The simulation was carried out for a time-invariant feedback path. Using the perceptual audio coding techniques based on masking capabilities of the auditory system in humans, a probe noise signal can be generated that is imperceptible in the presence of the loudspeaker signal [19]. For our simulations, we used a random white noise signal which was uncorrelated with the loudspeaker signal. This random white noise signal was shaped according to the thresholds estimated by the spectral masking model presented in [22] for the loudspeaker signal $q(n)$ in Fig. 1 and that for the loudspeaker signal of the basic adaptive feedback cancellation system with probe noise. Using these estimated masking thresholds as the basis, a shaping filter of order 127 for the proposed feedback canceller in Fig. 1 and a shaping filter of order 119 for the basic AFC with probe noise was created using the frequency sampling technique of FIR filter design. We verified the inaudibility of these perceptually-shaped probe signals by evaluating the loudspeaker output with added perceptually-shaped probe noise using the MATLAB implementation of the PESQ algorithm provided in [23]. Table 3 presents the explanation of the PESQ score of the audio signal. The PESQ value computed for the loudspeaker signal with perceptually-shaped probe signal for the linear prediction-based feedback canceller with shaped probe noise was 3.98, which according to Table 3, is very close to being 'perceptible but not annoying'. For the basic AFC with probe noise, the PESQ value was computed as 3.562, which lies between 'slightly annoying' and 'perceptible but not annoying'. Thus, a loudspeaker signal with satisfactorily imperceptible shaped probe noise signal was generated making it

possible to simulate both the above mentioned feedback cancellers with probe noise.

Spectrogram of the original speech signal without the effect of feedback is presented in Fig. 8 (a). The spectrogram for the loudspeaker signal of the basic AFC with probe noise is presented in Fig. 8 (b) and that of the loudspeaker signal for the linear prediction-based feedback canceller with shaped probe noise is presented in Fig. 8 (c). Signal formants are preserved in both Figs. 8 (b) and 8 (c). However, it can be seen from Fig. 8 (b) that there is distortion and whistling between 2 kHz to 6 kHz due to the presence of correlation between the input acoustic signal and the loudspeaker signal at high frequencies. Comparing Figs. 8 (c) and 8 (b), it can be observed in Fig. 8(c) that the distortion, along with whistling, is reduced between 2 kHz to 6 kHz due to the presence of BLPC vocoder that further reduces the high-frequency correlation between the loudspeaker signal and the incoming desired acoustic signal [6].

Further more, we computed the PSD estimates of the incoming acoustic signal $x(n)$ and the loudspeaker signal $q(n)$ and inserted them in the expressions in (C.2) and (C.9) to obtain prediction values for the PTF for speech signal as input. The true PTF values were computed according to the expression in (15). Figure 9 shows the simulation for the linear prediction-based feedback canceller with shaped probe noise at frequency bin $m = 12$ for the speech signal as input. It can be seen from the figure that the simulation curve is very close to the predicted convergence rate and the predicted steady-state value. Thus, the effectiveness of the proposed algorithm is verified in practical scenarios. Owing to the dynamic nature of the speech signal, variations are observed in the simulation curve of Fig. 9. The results presented in Figs. 5, 6 and 7 are averaged over 100 simulation runs of $2\text{x}10^4$ iterations each and are smoother as compared to that in Fig. 9, which has been averaged for only 5 simulation runs of approximately 120 seconds. Hence, the derived expressions are verified for speech input to the linear prediction-based feedback canceller with shaped probe signal.

## 7. Conclusion

We have analysed the linear prediction-based AFC system with and without probe noise, and derived approximate expressions for their PTFs. We have used these expressions to predict the performance of both the aforementioned feedback cancellation schemes on the basis of their rate of convergence, steady-state behaviour and stability constraint. The expressions derived for the rate of convergence and the steady-state error describe the effect of the overall system parameters and the adaptive algorithm on the system performance. Also, we have used the PTF approximate expressions for controlling the step size for the NLMS algorithm and the forgetting factor for the RLS algorithm for achieving the desired rate of convergence or steady-state behaviour at a particular frequency level. Our analysis has shown that the cost of achieving an unbiased feedback cancellation using linear prediction-based AFC system with shaped probe noise is an increase in the steady-state error by the ratio $S_q(\omega)/S_{\mathrm{p}}(\omega)$ in comparison to the feedback canceller without probe noise, when RLS algorithm is used. However, for NLMS algorithm, the cost of an unbiased feedback estimate is a reduction in the rate of convergence, along with an increase in the tracking error, by the ratio $S_q(\omega)/S_{\mathrm{p}}(\omega)$. A comparison of the linear prediction based feedback canceller with shaped probe noise and the basic feedback canceller with probe noise was also done based on spectrograms of the respective loudspeaker outputs. The loudspeaker output of the former had less distortion and whistling problem as compared to that of the latter. Finally, it has been observed and verified from the resulting simulations that the expressions derived provide an accurate approximation of the PTF, rate of convergence and steady-state error for a synthetic signal and speech signal as input, despite the assumptions made during the analysis.

As part of future research, we aim to improve upon the observed drawbacks for feedback cancellation with shaped probe noise in a linear prediction-based framework. Moreover, we also wish to use a variable-tap-length adaptive filter in the proposed feedback canceller and analyse its feedback cancellation perfor-

mance in a high-noise environment in terms of the PTF criterion.

**Acknowledgment**

This work is funded by the European Union's Seventh Framework Programme (FP7/2007-2013) under the Grant agreement number ITN-GA-2012-316969. The authors would like to thank Prof. Toon van Waterschoot (KU Leuven, Belgium) for his valuable suggestions throughout this work.

## 8. References

### References

[1] S. F. Lybarger, Acoustic feedback control, The Vanderbilt Hearing-Aid Report (1982) 87–90.

[2] J. M. Kates, Adaptive Feedback Cancellation in Hearing Aids, Springer Berlin Heidelberg, Berlin, Heidelberg, 2003, pp. 23–57.

[3] B. Rafaely, M. Roccasalva-Firenze, Control of feedback in hearing aids-a robust filter design approach, IEEE Transactions on Speech and Audio Processing 8 (6) (2000) 754–756.

[4] J. Hellgren, T. Lunner, S. Arlinger, System identification of feedback in hearing aids, The Journal of the Acoustical Society of America 105 (6) (1999) 3481–3496. doi:10.1121/1.424674.

[5] A. Spriet, S. Doclo, M. Moonen, J. Wouters, Feedback control in hearing aids, in: Springer handbook of speech processing, Springer, 2008, pp. 979–1000.

[6] G. Ma, F. Gran, F. Jacobsen, F. T. Agerkvist, Adaptive feedback cancellation with band-limited {LPC} vocoder in digital hearing aids, IEEE Transactions on Audio, Speech, and Language Processing 19 (4) (2011) 677–687. doi:10.1109/TASL.2010.2057245.

[7] A. Anand, A. Kar, M. N. S. Swamy, Design and analysis of a {BLPC} vocoder-based adaptive feedback cancellation with probe noise, Applied Acoustics 115 (2017) 196 – 208. doi:https://doi.org/10.1016/j.apacoust.2016.08.023.

[8] M. Guo, Analysis, design, and evaluation of acoustic feedback cancellation systems for hearing aids, Ph.D. thesis, PhD dissertation, Department of Electronic Systems, Aalborg University (2012).

[9] H. Dillon, Hearing aids, Boomerang press Sydney, Australia, 2001.

[10] B. Moore, An Introduction to the Psychology of Hearing, Brill, 2012.

[11] S. S. Haykin, Adaptive filter theory, Prentice-Hall information and system sciences series, Prentice Hall, 1991.
URL https://books.google.co.in/books?id=E5hTAAAAMAAJ

[12] M. Guo, T. B. Elmedyb, S. H. Jensen, J. Jensen, Analysis of acoustic feedback/echo cancellation in multiple-microphone and single-loudspeaker systems using a power transfer function method, Signal Processing, IEEE Transactions on 59 (12) (2011) 5774–5788.

[13] M. Guo, S. H. Jensen, J. Jensen, Novel acoustic feedback cancellation approaches in hearing aid applications using probe noise and probe noise enhancement, IEEE Transactions on Audio, Speech, and Language Processing 20 (9) (2012) 2549–2563. doi:10.1109/TASL.2012.2206025.

[14] S. Gunnarsson, L. Ljung, Frequency domain tracking characteristics of adaptive algorithms, IEEE Transactions on Acoustics, Speech, and Signal Processing 37 (7) (1989) 1072–1089. doi:10.1109/29.32284.

[15] V. Krishnan, Probability and Random Processes, Wiley Survival Guides in Engineering and Science, Wiley, 2006.
URL https://books.google.co.in/books?id=ckklgif1M68C

[16] H. Nyquist, Regeneration theory, Bell System Technical Journal 11 (1) (1932) 126–147. doi:10.1002/j.1538-7305.1932.tb02344.x.
URL http://dx.doi.org/10.1002/j.1538-7305.1932.tb02344.x

[17] S. Gunnarsson, On the quality of recursively identified fir models, IEEE Transactions on Signal Processing 40 (3) (1992) 679–682. doi:10.1109/78.120811.

[18] C. R. C. Nakagawa, Control of feedback for assistive listening devices, Ph.D. thesis, PhD dissertation, School of Electrical and Computer Engineering, Curtin University (2014).

[19] T. Painter, A. Spanias, Perceptual coding of digital audio, Proceedings of the IEEE 88 (4) (2000) 451–515.

[20] T. van Waterschoot, M. Moonen, Fifty years of acoustic feedback control: State of the art and future challenges, Proceedings of the IEEE 99 (2) (2011) 288–327. doi:10.1109/JPROC.2010.2090998.

[21] A. Spriet, I. Proudler, M. Moonen, J. Wouters, Adaptive feedback cancellation in hearing aids with linear prediction of the desired signal, IEEE Transactions on Signal Processing 53 (10) (2005) 3749–3763. doi:10.1109/TSP.2005.855108.

[22] J. D. Johnston, Transform coding of audio signals using perceptual noise criteria, IEEE Journal on Selected Areas in Communications 6 (2) (1988) 314–323. doi:10.1109/49.608.

[23] P. Loizou, Speech Enhancement: Theory and Practice, Second Edition, Taylor & Francis, 2013.
URL https://books.google.co.in/books?id=ntXLfZkuGTwC

[24] H. J. Kushner, Approximation and weak convergence methods for random processes, with applications to stochastic systems theory, Cambridge, Mass. : MIT Press, 1984, includes index.

[25] R. M. Gray, et al., Toeplitz and circulant matrices: A review, Foundations and Trends in Communications and Information Theory 2 (3) (2006) 155–239.

## Figure Captions

1 Linear prediction-based AFC system with shaped probe noise signal

2 Linear prediction-based AFC system without probe noise [6]

3 Magnitude response of the original feedback path

4 Frequency Response of the high-pass filter $H_{\mathrm{p}}(k)$ and the low-pass filter $L_{\mathrm{p}}(k)$

5 Simulation results for linear prediction-based feedback canceller (a) with shaped probe noise and (b) without probe noise for the frequency bin $m = 7$

6 Simulation results for linear prediction-based feedback canceller (a) with shaped probe noise and (b) without probe noise for the frequency bin $m = 12$

7 Simulation result for linear prediction-based feedback canceller with shaped probe noise for the desired steady-state error of -0.015 dB per iterative instant $n$

8 Spectrogram for (a) Speech input. (b) Loudspeaker output of the basic AFC with probe noise in [8, 18]. (c) Loudspeaker output of the linear prediction-based feedback canceller with shaped probe noise

9 Simulation runs for linear prediction-based feedback canceller with shaped probe signal when speech signal is used as input $m = 12$

# Table Captions

1 Summary of the influence of the parameters of RLS and NLMS algorithms on the behaviour of proposed feedback cancellation design with shaped probe noise

2 Summary of the influence of the parameters of RLS and NLMS algorithms on the behaviour of the linear prediction-based AFC system without probe noise

3 Explanation of PESQ values

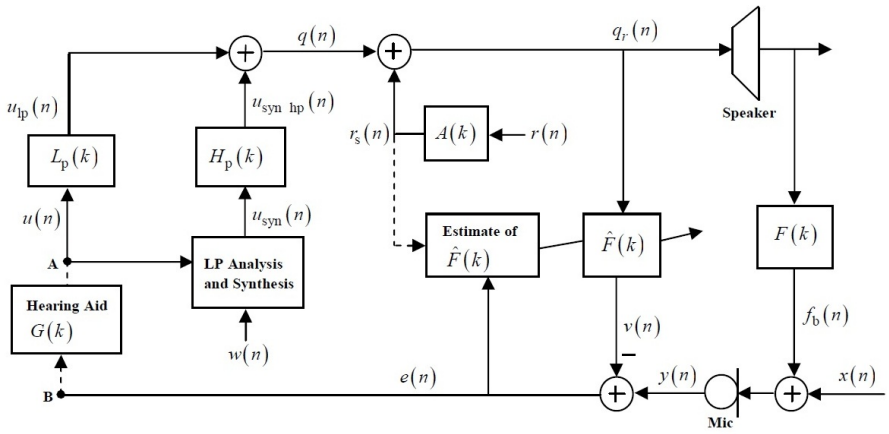


Figure 1: Linear prediction-based AFC system with shaped probe noise signal

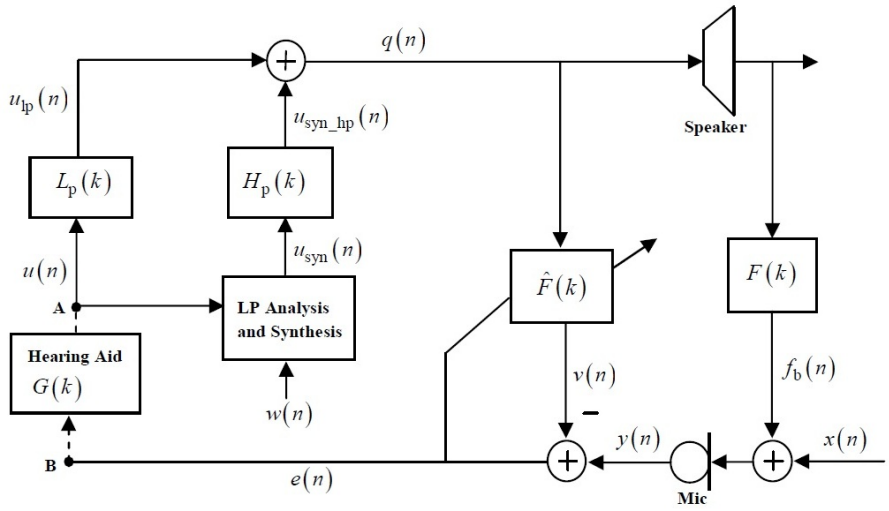


Figure 2: Linear prediction-based AFC system without probe noise [6]

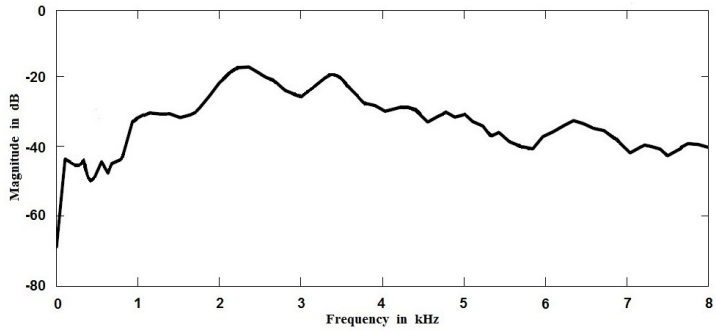


Figure 3: Magnitude response of the original feedback path

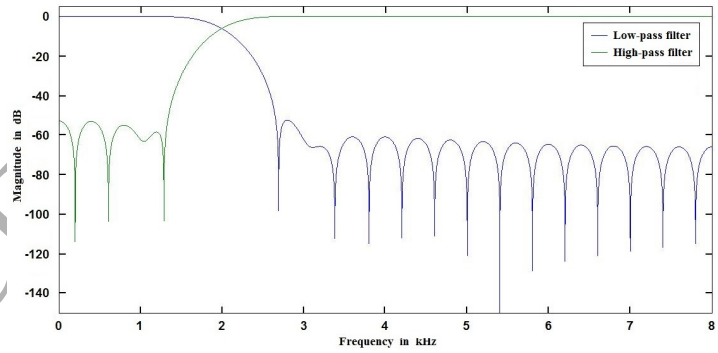


Figure 4: Frequency Response of the high-pass filter $H_{\mathrm{p}}(k)$ and the low-pass filter $L_{\mathrm{p}}(k)$

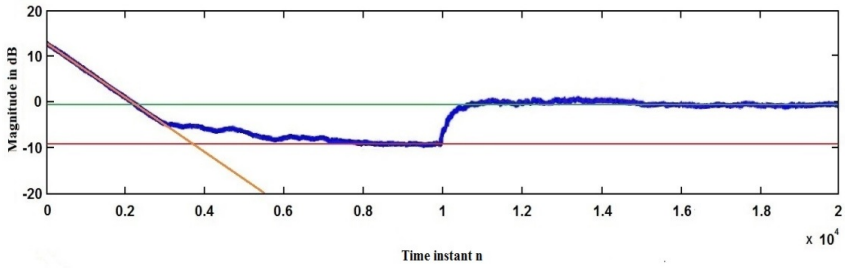


(a)

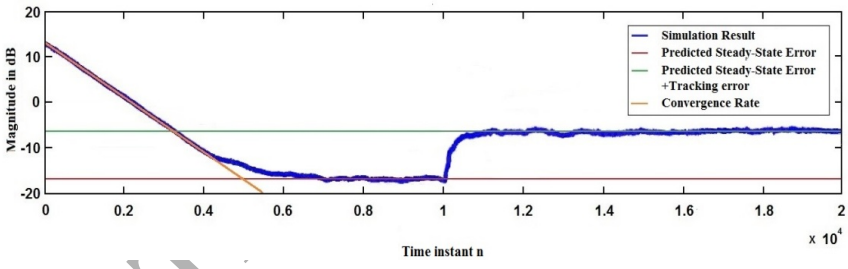


(b)

Figure 5: Simulation results for linear prediction-based feedback canceller (a) with shaped probe noise and (b) without probe noise for the frequency bin $m = 7$

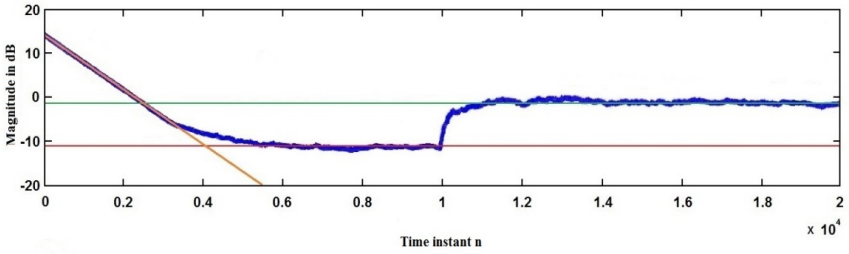


(a)

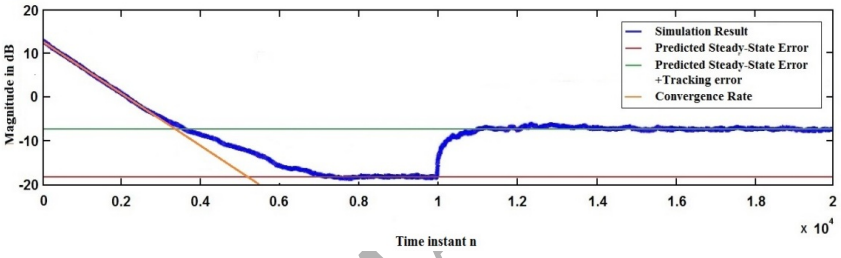


(b)

Figure 6: Simulation results for linear prediction-based feedback canceller (a) with shaped probe noise and (b) without probe noise for the frequency bin $m = 12$

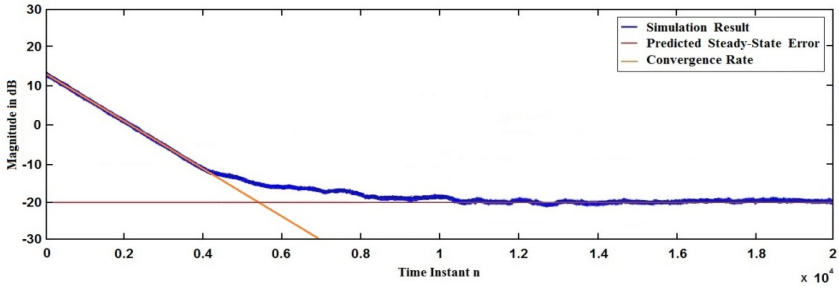


Figure 7: Simulation result for linear prediction-based feedback canceller with shaped probe noise for the desired steady-state error of -0.015 dB per iterative instant $n$

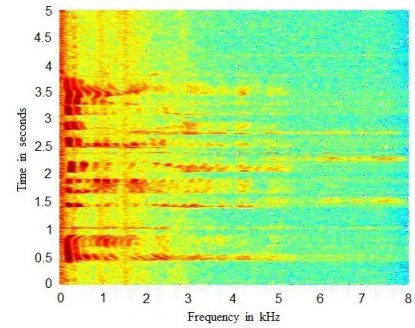


(a)

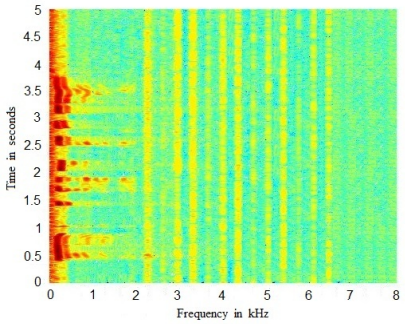


(b)

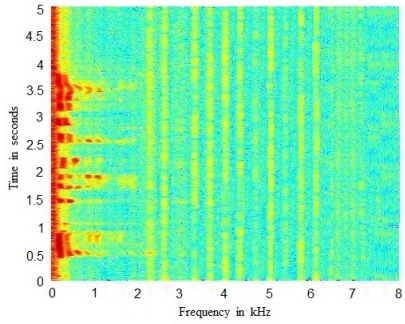


(c)

Figure 8: Spectrogram for (a) Speech input. (b) Loudspeaker output of the basic AFC with probe noise in [8, 18]. (c) Loudspeaker output of the linear prediction-based feedback canceller with shaped probe noise

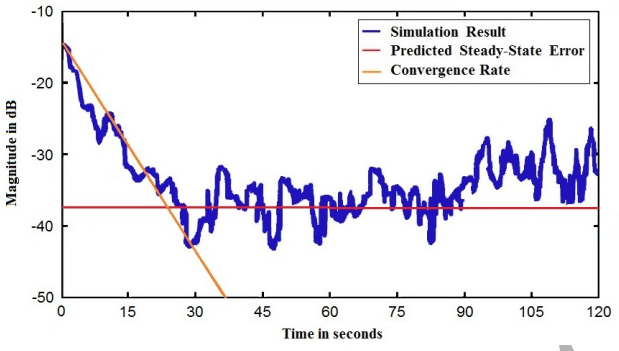


Figure 9: Simulation runs for linear prediction-based feedback canceller with shaped probe signal when speech signal is used as input $m = 12$

Table 1: Summary of the influence of the parameters of RLS and NLMS algorithms on the behaviour of proposed feedback cancellation design with shaped probe noise

| Algorithm/parameters | CR | SSE | TE |
|---|---|---|---|
| RLS Algorithm | | | |
| $\lambda$ | IP (25) | IP (28) | DP (28) |
| $L_f$ | - | DP (28) | - |
| $S_q(\omega)$ | - | - | - |
| $S_p(\omega)$ | - | IP (28) | |
| $S_x(\omega)$ | - | DP (28) | - |
| $S_{\underset{\sim}{f}}(\omega)$ | - | - | DP (28) |
| $\lvert A(\omega)\rvert^2$ | - | IP (28) | - |
| NLMS Algorithm | | | |
| $\tilde{\mu}(n)$ | DP (24, 39) | DP (42) | IP (42) |
| $\frac{L_f}{(\delta+L_f\,\sigma_{\mathrm{p}}^2)}$ | - | DP (42) | - |
| $\frac{S_{\mathrm{p}}(\omega)}{(\delta+L_f\,\sigma_{\mathrm{p}}^2)}$ | DP (24, 39) | - | IP (42) |
| $S_x(\omega)$ | - | DP (42) | - |
| $S_{\underset{\sim}{f}}(\omega)$ | - | - | DP (42) |
| $\lvert A(\omega)\rvert^2$ | DP (24, 39) | - | IP (42) |

(DP: Directly proportional, IP: Inversely proportional)

Table 2: Summary of the influence of the parameters of RLS and NLMS algorithms on the behaviour of the linear prediction-based AFC system without probe noise

| Algorithm/parameters | CR | SSE | TE |
|---|---|---|---|
| RLS Algorithm | | | |
| $\lambda$ | IP (25) | IP (C.11) | DP (C.11) |
| $L_f$ | - | DP (C.11) | - |
| $S_q(\omega)$ | - | IP (C.11) | - |
| $S_x(\omega)$ | - | DP (C.11) | - |
| $S_{\breve{f}}(\omega)$ | - | - | DP (C.11) |
| NLMS Algorithm | | | |
| $\tilde{\mu}(n)$ | DP (24, D.6) | DP (D.9) | IP (D.9) |
| $\frac{L_f}{(\delta+L_f\,\sigma_q^2)}$ | - | DP (D.9) | - |
| $\frac{S_q(\omega)}{(\delta+L_f\,\sigma_q^2)}$ | DP (24, D.6) | - | IP (D.9) |
| $S_x(\omega)$ | - | DP (D.9) | - |
| $S_{\breve{f}}(\omega)$ | - | - | DP (D.9) |

(DP: Directly proportional, IP: Inversely proportional)

Table 3: Explanation of PESQ values

| **PESQ value** | **Signal Quality** | **Comments on impairment** |
|---|---|---|
| 1 | Poor | Very annoying |
| 2 | Bad | Annoying |
| 3 | Fair | Slightly annoying |
| 4 | Good | Perceptible but not annoying |
| 5 | Excellent | Imperceptible |

## Appendix A.

*Proof of Theorem 1*

*Proof.* Using the shaped-probe-noise approach for feedback path estimation, the microphone signal in (5) can be rewritten as

$$y(n) = x(n) + F(k, n-1)\, q_r(n). \tag{A.1}$$

Rewriting (6), we have

$$e(n) = y(n) - \hat{F}(k, n-1)\, q_r(n). \tag{A.2}$$

Combining (10) with (A.1) and substituting into (A.2), we get

$$\begin{aligned} e(n) &= x(n) + F(k, n-1)\, q_r(n) - \hat{F}(k, n-1)\, q_r(n) \\ &= x(n) - \Big(\hat{F}(k, n-1) - F(k, n-1)\Big)\, q(n) - \Big(\hat{F}(k, n-1) - F(k, n-1)\Big)\, r_{\mathrm{s}}(n). \end{aligned} \tag{A.3}$$

Rewriting (4) in the frequency domain and substituting into (A.3), we have

$$e(n) = x(n) - \tilde{F}(k, n-1)\, q(n) - \tilde{F}(k, n-1)\, r_{\mathrm{s}}(n). \tag{A.4}$$

The RLS weight update equation for the feedback path estimation filter $\tilde{F}(k)$ in Fig. 1 is given as [11]

$$\hat{\mathbf{f}}(n) = \hat{\mathbf{f}}(n-1) + \mathbf{D}(n)\, \mathbf{r}_{\mathrm{s}}(n)\, e(n), \tag{A.5}$$

where

$$\mathbf{D}(n) = \frac{\mathbf{R}^{-1}(n-1)}{\lambda + \mathbf{r}_{\mathrm{s}}{}^{T}(n)\, \mathbf{R}^{-1}(n-1)\, \mathbf{r}_{\mathrm{s}}(n)}, \tag{A.6}$$

and $\lambda$ denotes the forgetting factor such that $0 < \lambda \leq 1$. In (A.6), $\mathbf{R}(n)$ is the $L_{\hat{f}} \times L_{\hat{f}}$ input auto-correlation matrix which can be computed recursively as

$$\mathbf{R}(n) = \lambda \mathbf{R}(n-1) - \mathbf{r}_{\mathrm{s}}(n)\, \mathbf{r}_{\mathrm{s}}{}^{T}(n). \tag{A.7}$$

In order to compute the filter coefficients of the adaptive filter, a recursive expression for $\mathbf{R}^{-1}(n)$ is required in terms of $\mathbf{R}^{-1}(n-1)$ [11]. Using matrix inversion lemma [10], $\mathbf{R}^{-1}(n)$ can be obtained from (A.7) as

$$\mathbf{R}^{-1}(n) = \lambda^{-1}\Big[\mathbf{R}^{-1}(n-1) - \mathbf{D}(n)\, \mathbf{r}_{\mathrm{s}}(n)\, \mathbf{r}_{\mathrm{s}}^{T}(n)\, \mathbf{R}^{-\mathbf{1}}(\mathbf{n}-\mathbf{1})\Big]. \tag{A.8}$$

In (A.8), $\mathbf{R}^{-1}(0) = \delta \mathbf{I}$, where $\mathbf{I}$ is an identity matrix and the regularization parameter $\delta$ is a positive real number such that $\mathbf{R}(n)$ does not become singular for a small value of $n$ [11]. Substituting the combination of (3), (4) and (A.4) into (A.5), we get

$$\tilde{\mathbf{f}}(n) = \left[\mathbf{I} - \mathbf{D}(n)\,\mathbf{r}_{\mathrm{s}}(n)\,\mathbf{q}^{T}(n) - \mathbf{D}(n)\,\mathbf{r}_{\mathrm{s}}(n)\,\mathbf{r}_{\mathrm{s}}{}^{T}(n)\right]\tilde{\mathbf{f}}(n-1) + \mathbf{D}(n)\,\mathbf{r}_{\mathrm{s}}(n)\,x(n) - \breve{\mathbf{f}}(n). \tag{A.9}$$

For further analysis, we consider the estimation-error covariance matrix

$$\bar{\mathbf{F}}(n) = E\left[\tilde{\mathbf{f}}(n)\,\tilde{\mathbf{f}}^{T}(n)\right]. \tag{A.10}$$

In order to compute $\bar{\mathbf{F}}(n)$ from (A.10), $\breve{\mathbf{f}}(n)$ is assumed to be uncorrelated with all the other terms in (A.9) $\big($assumption (v)$\big)$. Substituting (A.9) into (A.10), we have

$$\begin{aligned}
\bar{\mathbf{F}}(n) = E\Big[&\tilde{\mathbf{f}}(n-1)\,\tilde{\mathbf{f}}^{T}(n-1) - \tilde{\mathbf{f}}(n-1)\,\tilde{\mathbf{f}}^{T}(n-1)\,\mathbf{q}(n)\,\mathbf{r}_{\mathrm{s}}^{T}(n)\,\mathbf{D}(n)\\
&- \tilde{\mathbf{f}}(n-1)\,\tilde{\mathbf{f}}^{T}(n-1)\,\mathbf{r}_{\mathrm{s}}(n)\,\mathbf{r}_{\mathrm{s}}^{T}(n)\,\mathbf{D}(n) + \tilde{\mathbf{f}}(n-1)\,x(n)\,\mathbf{q}^{T}(n)\,\mathbf{D}(n)\\
&- \mathbf{D}(n)\,\mathbf{r}_{\mathrm{s}}(n)\,\mathbf{q}^{T}(n)\,\tilde{\mathbf{f}}(n-1)\,\tilde{\mathbf{f}}^{T}(n-1)\\
&+ \mathbf{D}(n)\,\mathbf{r}_{\mathrm{s}}(n)\,\mathbf{q}^{T}(n)\,\tilde{\mathbf{f}}(n-1)\,\tilde{\mathbf{f}}^{T}(n-1)\,\mathbf{q}(n)\,\mathbf{r}_{\mathrm{s}}^{T}(n)\,\mathbf{D}(n)\\
&- \mathbf{D}(n)\,\mathbf{r}_{\mathrm{s}}(n)\,\mathbf{q}^{T}(n)\,\tilde{\mathbf{f}}(n-1)\,x(n)\,\mathbf{q}^{T}(n)\,\mathbf{D}(n)\\
&+ \mathbf{D}(n)\,\mathbf{r}_{\mathrm{s}}(n)\,\mathbf{q}^{T}(n)\,\tilde{\mathbf{f}}(n-1)\,\tilde{\mathbf{f}}^{T}(n-1)\,\mathbf{r}_{\mathrm{s}}(n)\,\mathbf{r}_{\mathrm{s}}^{T}(n)\,\mathbf{D}(n)\\
&- \mathbf{D}(n)\,\mathbf{r}_{\mathrm{s}}(n)\,\mathbf{r}_{\mathrm{s}}^{T}(n)\,\tilde{\mathbf{f}}(n-1)\,\tilde{\mathbf{f}}^{T}(n-1)\\
&+ \mathbf{D}(n)\,\mathbf{r}_{\mathrm{s}}(n)\,\mathbf{r}_{\mathrm{s}}^{T}(n)\,\tilde{\mathbf{f}}(n-1)\,\tilde{\mathbf{f}}^{T}(n-1)\,\mathbf{q}(n)\,\mathbf{r}_{\mathrm{s}}^{T}(n)\,\mathbf{D}(n)\\
&- \mathbf{D}(n)\,\mathbf{r}_{\mathrm{s}}(n)\,\mathbf{r}_{\mathrm{s}}^{T}(n)\,\tilde{\mathbf{f}}(n-1)\,x(n)\,\mathbf{q}^{T}(n)\,\mathbf{D}(n)\\
&+ \mathbf{D}(n)\,\mathbf{r}_{\mathrm{s}}(n)\,\mathbf{r}_{\mathrm{s}}^{T}(n)\,\tilde{\mathbf{f}}(n-1)\,\tilde{\mathbf{f}}^{T}(n-1)\,\mathbf{r}_{\mathrm{s}}(n)\,\mathbf{r}_{\mathrm{s}}^{T}(n)\,\mathbf{D}(n)\\
&+ \mathbf{D}(n)\,\mathbf{q}(n)\,x(n)\,\tilde{\mathbf{f}}^{T}(n-1) - \mathbf{D}(n)\,\mathbf{q}(n)\,x(n)\,\tilde{\mathbf{f}}^{T}(n-1)\,\mathbf{q}(n)\,\mathbf{r}_{\mathrm{s}}^{T}(n)\,\mathbf{D}(n)\\
&+ \mathbf{D}(n)\,\mathbf{q}(n)\,x(n)\,x(n)\,\mathbf{q}^{T}(n)\,\mathbf{D}(n)\\
&- \mathbf{D}(n)\,\mathbf{q}(n)\,x(n)\,\tilde{\mathbf{f}}^{T}(n-1)\,\mathbf{r}_{\mathrm{s}}(n)\,\mathbf{r}_{\mathrm{s}}^{T}(n)\,\mathbf{D}(n) + \breve{\mathbf{f}}(n)\,\breve{\mathbf{f}}^{T}(n)\Big].
\end{aligned} \tag{A.11}$$

To represent (A.11) in a simplified form, let us represent a matrix $\boldsymbol{\Delta}(n)$ such that

$$\boldsymbol{\Delta}(n) = \mathbf{I} - \mathbf{D}(n)\,\mathbf{r}_{\mathrm{s}}(n)\,\mathbf{q}^{T}(n) - \mathbf{D}(n)\,\mathbf{r}_{\mathrm{s}}(n)\,\mathbf{r}_{\mathrm{s}}{}^{T}(n). \tag{A.12}$$

Collecting terms in (A.11), substituting (A.12) into (A.11) and using assumption (iv), we get

$$\begin{aligned}\bar{\mathbf{F}}(n) =& \bar{\mathbf{F}}(n-1) - \mathbf{D}(n)\,\mathbf{r}_{\mathrm{s}}(n)\,\mathbf{r}_{\mathrm{s}}{}^{T}(n)\,\bar{\mathbf{F}}(n-1) \\ &- \bar{\mathbf{F}}(n-1)\,\mathbf{r}_{\mathrm{s}}(n)\,\mathbf{r}_{\mathrm{s}}{}^{T}(n)\,\mathbf{D}(n) + \breve{\mathbf{F}}(n) \\ &+ \mathbf{D}(n)\,\mathbf{r}_{\mathrm{s}}(n)\,\mathbf{r}_{\mathrm{s}}{}^{T}(n)\,\mathbf{R}_{x}(0)\,\mathbf{D}(n) + E\left[\mathbf{D}(n)\,\mathbf{r}_{\mathrm{s}}(n)\,x(n)\,\tilde{\mathbf{f}}^{T}(n-1)\right] \\ &+ E\left[\tilde{\mathbf{f}}(n-1)\,x(n)\,\mathbf{r}_{\mathrm{s}}{}^{T}(n)\,\mathbf{D}(n)\right] - \bar{\mathbf{F}}(n-1)\,\mathbf{q}(n)\,\mathbf{r}_{\mathrm{s}}^{T}(n)\,\mathbf{D}(n) \\ &- \mathbf{D}(n)\,\mathbf{r}_{\mathrm{s}}(n)\,\mathbf{q}^{T}(n)\,\bar{\mathbf{F}}(n-1) \\ &+ \mathbf{D}(n)\,\mathbf{r}_{\mathrm{s}}(n)\,\mathbf{q}^{T}(n)\,\bar{\mathbf{F}}(n-1)\,\mathbf{r}_{\mathrm{s}}(n)\,\mathbf{r}_{\mathrm{s}}^{T}(n)\,\mathbf{D}(n) \\ &+ \mathbf{D}(n)\,\mathbf{r}_{\mathrm{s}}(n)\,\mathbf{q}^{T}(n)\,\bar{\mathbf{F}}(n-1)\,\mathbf{q}(n)\,\mathbf{r}_{\mathrm{s}}^{T}(n)\,\mathbf{D}(n), \end{aligned} \tag{A.13}$$

where $\breve{\mathbf{F}}(n) = E\left[\breve{\mathbf{f}}(n)\ \ \breve{\mathbf{f}}^{T}(n)\right]$ is the feedback path variation vector covariance matrix. It can be seen that (A.13) is a difference equation in terms of $\bar{\mathbf{F}}(n)$. According to the direct averaging method [14, 24], the term $\mathbf{r}_{\mathrm{s}}(n)\,\mathbf{r}_{\mathrm{s}}{}^{T}(n-m)$ can be replaced by its sample average as

$$\mathbf{R}_{\mathrm{p}}(m) = \lim_{N\to\infty}\frac{1}{N}\sum_{n=1}^{N}\mathbf{r}_{\mathrm{s}}(n)\,\mathbf{r}_{\mathrm{s}}{}^{T}(n-m), \tag{A.14}$$

where $m$ is the time delay. Similarly, the term $\mathbf{r}_{\mathrm{s}}(n)\,\mathbf{q}^{T}(n-m)$ can be replaced by its sample average which can be expressed using assumption (i) as

$$\mathbf{R}_{rq}(m) = \lim_{N\to\infty}\frac{1}{N}\sum_{n=1}^{N}\mathbf{r}_{\mathrm{s}}(n)\,\mathbf{q}^{T}(n-m) = 0. \tag{A.15}$$

Combining (A.14) and (A.15) for $m = 0$, and substituting into (A.13), we get the approximate feedback estimation-error covariance matrix as

$$\begin{aligned}\bar{\mathbf{F}}_{\mathrm{a}}(n) =& \bar{\mathbf{F}}_{\mathrm{a}}(n-1) - \mathbf{D}(n)\,\mathbf{R}_{\mathrm{p}}(0)\,\bar{\mathbf{F}}_{\mathrm{a}}(n-1) - \bar{\mathbf{F}}_{\mathrm{a}}(n-1)\,\mathbf{R}_{\mathrm{p}}(0)\,\mathbf{D}(n) + \breve{\mathbf{F}}(n) \\ &+ \mathbf{D}(n)\,\mathbf{R}_{\mathrm{p}}(0)\,\mathbf{R}_{x}(0)\,\mathbf{D}(n) + E\left[\mathbf{D}(n)\,\mathbf{r}_{\mathrm{s}}(n)\,x(n)\,\tilde{\mathbf{f}}^{T}(n-1)\right] \\ &+ E\left[\tilde{\mathbf{f}}(n-1)\,x(n)\,\mathbf{r}_{\mathrm{s}}^{T}(n)\,\mathbf{D}(n)\right]. \end{aligned} \tag{A.16}$$

Further, there is a need to evaluate the terms $E\left[\mathbf{D}(n)\,\mathbf{r}_{\mathrm{s}}(n)\,x(n)\,\tilde{\mathbf{f}}^{T}(n-1)\right]$ and $E\left[\tilde{\mathbf{f}}(n-1)\,x(n)\,\mathbf{r}_{\mathrm{s}}^{T}(n)\,\mathbf{D}(n)\right]$ in (A.16) to obtain the final expression for

$\bar{\mathbf{F}}_{\mathrm{a}}(n)$. The evaluation of both the terms is presented in Appendix B in detail. Finally, we have

$$\bar{\mathbf{F}}_{\mathrm{a}}(n) = \bar{\mathbf{F}}_{\mathrm{a}}(n-1) - \mathbf{D}(n)\,\mathbf{R}_{r_{\mathrm{s}}}(0)\,\bar{\mathbf{F}}_{\mathrm{a}}(n-1) - \bar{\mathbf{F}}_{\mathrm{a}}(n-1)\,\mathbf{R}_{\mathrm{p}}(0)\,\mathbf{D}(n) + \breve{\mathbf{F}}(n) + \mathbf{D}(n)\,\mathbf{D}^{T}(n)\sum_{t=-t_0}^{t_0}\mathbf{R}_{\mathrm{p}}(t)\,r_x(t). \tag{A.17}$$

In (15), the expression for $\zeta(\omega, n)$ contains $\tilde{F}(\omega, n)$, which is the frequency response of $\tilde{\mathbf{f}}(n)$. In order to find an expression for $\hat{\zeta}(\omega, n)$, let $\mathbf{\Gamma}$ be an $L_f \times L_f$ DFT matrix such that $\mathbf{\Gamma}$ is a complex quantity. Then, we can say that $\mathbf{\Gamma}$ diagonalizes a Toeplitz matrix asymptotically as $L_f \to \infty$ [14, 25]. Therefore, diagonalizing $\bar{\mathbf{F}}_{\mathrm{a}}(n)$ using $\mathbf{\Gamma}$, we obtain

$$\hat{\boldsymbol{\chi}}(n) = \mathbf{\Gamma}\;\bar{\mathbf{F}}_{\mathrm{a}}(n)\;\mathbf{\Gamma}^{H}. \tag{A.18}$$

Here, $\hat{\boldsymbol{\chi}}(n)$ approaches a diagonal matrix as $L_f \to \infty$ and has diagonal elements expressed by $\hat{\zeta}(\omega, n)$. Substituting (A.17) into (A.18), we have

$$\begin{aligned}\hat{\boldsymbol{\chi}}(n) = {} & \mathbf{\Gamma}\;\bar{\mathbf{F}}_{\mathrm{a}}(n-1)\;\mathbf{\Gamma}^{H} + \mathbf{\Gamma}\;\breve{\mathbf{F}}(n)\;\mathbf{\Gamma}^{H} - \mathbf{D}(n)\;\frac{1}{L_f}\mathbf{\Gamma}\,\mathbf{R}_{\mathrm{p}}(0)\;\mathbf{\Gamma}^{H}\,\mathbf{\Gamma}\,\bar{\mathbf{F}}_{\mathrm{a}}(n-1)\;\mathbf{\Gamma}^{H} \\ & - \frac{1}{L_f}\mathbf{\Gamma}\,\bar{\mathbf{F}}_{\mathrm{a}}(n-1)\;\mathbf{\Gamma}^{H}\mathbf{\Gamma}\,\mathbf{R}_{\mathrm{p}}(0)\;\mathbf{\Gamma}^{H}\mathbf{D}(n) \\ & + \mathbf{D}(n)\,\mathbf{D}^{T}(n)\sum_{t=-t_0}^{t_0}\mathbf{\Gamma}\,\mathbf{R}_{\mathrm{p}}(t)\;\mathbf{\Gamma}^{H} r_x(t).\end{aligned} \tag{A.19}$$

In (A.19), the matrix $\breve{\mathbf{F}}(n)$ is diagonalized as $\mathbf{\Gamma}\,\breve{\mathbf{F}}(n)\;\mathbf{\Gamma}^{H}$ having diagonal elements $S_{\breve{f}}(\omega)$. Similarly, the matrix $\mathbf{R}_{\mathrm{p}}(0)$ is diagonalized as $\frac{1}{L_f}\;\mathbf{\Gamma}\;\mathbf{R}_{\mathrm{p}}(0)\;\mathbf{\Gamma}^{H}$ having diagonal elements $S_{\mathrm{p}}(\omega)$, which is the PSD of $r_{\mathrm{s}}(n)$ and is defined as the Fourier transform of the auto-correlation function of $r_{\mathrm{s}}(n)$. We can express $S_{\mathrm{p}}(\omega)$ as

$$S_{\mathrm{p}}(\omega) = |A(\omega)|^2 S_r(\omega), \tag{A.20}$$

where $A(\omega)$ is the frequency response $A(k)$ and $S_r(\omega)$ is the PSD of unshaped probe noise $r(n)$. The PTF-approximation $\hat{\zeta}(\omega, n)$ forms the diagonal elements of the matrix $\hat{\boldsymbol{\chi}}(n)$. Therefore, replacing the terms $\hat{\boldsymbol{\chi}}(n)$, $\mathbf{\Gamma}\;\bar{\mathbf{F}}_{\mathrm{a}}(n-1)\;\mathbf{\Gamma}^{H}$,

$\frac{1}{L_f}\mathbf{\Gamma}\,\mathbf{R}_{\mathrm{p}}(0)\,\mathbf{\Gamma}^H$ and $\mathbf{\Gamma}\,\breve{\mathbf{F}}(n)\,\mathbf{\Gamma}^H$ in (A.19) with their respective diagonal elements, the expression for $\hat{\zeta}(\omega,n)$ can be written as

$$\begin{aligned}\hat{\zeta}(\omega,n) &= (1-2\,d(\omega,n)\,S_{\mathrm{p}}(\omega))\,\hat{\zeta}(\omega,n-1)\\ &\quad + L_f\;d^2(\omega,n)\;S_{\mathrm{p}}(\omega)\,S_x(\omega)+S_{\breve{f}}(\omega)\\ &= \left(1-2\,d(\omega,n)\,|A(\omega)|^2 S_r(\omega)\right)\hat{\zeta}(\omega,n-1)\\ &\quad + L_f\;d^2(\omega,n)\;|A(\omega)|^2 S_r(\omega)\,S_x(\omega)+S_{\breve{f}}(\omega)\,, \end{aligned}\tag{A.21}$$

where $d(\omega,n)$ is the diagonal entry of $\frac{1}{L_f}\,\mathbf{\Gamma}\,\mathbf{D}(n)\;\mathbf{\Gamma}^H$ (see Appendix B) expressed as

$$d(\omega,n)=\frac{1-\lambda}{S_{\mathrm{p}}(\omega)}=\frac{1-\lambda}{|A(\omega)|^2 S_r(\omega)}\,,\tag{A.22}$$

and $S_x(\omega)$ is the PSD of the incoming desired acoustic signal $x(n)$ and is defined as the Fourier transform of $r_x(m)$. Substituting (A.22) into (A.21), the PTF of (15) can be written approximately as (16). □

## Appendix B.

*Evaluation of the term* $E\left[\mathbf{D}(n)\,\mathbf{r}_s(n)\,x(n)\,\tilde{\mathbf{f}}^T(n-1)\right]$

We substitute (A.12) into (A.9) and rewrite the expression for $\tilde{\mathbf{f}}(n)$ as

$$\tilde{\mathbf{f}}(n)=\mathbf{\Delta}(n)\,\tilde{\mathbf{f}}(n-1)+\mathbf{D}(n)\,\mathbf{r}_{\mathrm{s}}(n)\,x(n)-\breve{\mathbf{f}}(n)\,.\tag{B.1}$$

Simplifying the expanded expression in (B.2), we get

$$\tilde{\mathbf{f}}(n) = \prod_{l=1}^{n} \mathbf{\Delta}(l)\tilde{\mathbf{f}}(0) + \sum_{m=1}^{n} \left[ \left( \prod_{l=m+1}^{n} \mathbf{\Delta}(l) \right) \left( \mathbf{D}(m)\, \mathbf{r}_{\mathrm{s}}(m)\, x(m) - \breve{\mathbf{f}}(m) \right) \right]. \quad \text{(B.3)}$$

In (B.3), it is assumed that the iteration for the adaptation process begins at $n = 0$ and also $\prod_{l=n_0}^{n} \mathbf{\Delta}(l) = \mathbf{I}\ \forall n_0 > n$. Substituting (B.3) into (A.16) for the term $E\left[\mathbf{D}(n)\, \mathbf{r}_{\mathrm{s}}(n)\, x(n)\, \tilde{\mathbf{f}}^T(n-1)\right]$, using assumption (iv) and considering $\tilde{\mathbf{f}}(0) = \hat{\mathbf{f}}(0) - \mathbf{f}(0)$ to be uncorrelated with $\mathbf{r}_{\mathrm{s}}(n)$, we have

$$\begin{aligned} & E\left[\mathbf{D}(n)\, \mathbf{r}_{\mathrm{s}}(n)\, x(n)\, \tilde{\mathbf{f}}^T(n-1)\right] \\ &= E\Bigg[\mathbf{D}(n)\, \mathbf{r}_{\mathrm{s}}(n)\, x(n) \Bigg( \prod_{l=1}^{n} \mathbf{\Delta}(l)\tilde{\mathbf{f}}(0) + \sum_{m=1}^{n} \Bigg( \prod_{l=m+1}^{n} \mathbf{\Delta}(l) \Bigg) \\ &\qquad \left[\mathbf{D}(m)\, \mathbf{r}_{\mathrm{s}}(m)\, x(m) - \breve{\mathbf{f}}(m)\right] \Bigg) \Bigg)^T \Bigg] \\ &= \sum_{t=-1}^{-(n-1)} \mathbf{D}(n)\, \mathbf{D}^T(n+t)\, \mathbf{r}_{\mathrm{s}}(n)\, \mathbf{r}_{\mathrm{s}}^T(n+t)\, r_x(t) \left( \prod_{l=n+1+t}^{n-1} \mathbf{\Delta}(l) \right)^T, \end{aligned} \quad \text{(B.4)}$$

where $t = m - n$. Since only the steady-state behaviour of the PTF is influenced by (B.4), we can consider a large value of $n$ for $n - 1 \geq t_0$ and rewrite (B.4) as

$$\begin{aligned} & E\left[\mathbf{D}(n)\, \mathbf{r}_{\mathrm{s}}(n)\, x(n)\, \tilde{\mathbf{f}}^T(n-1)\right] = \\ & \qquad \sum_{t=-1}^{-t_0} \mathbf{D}(n)\, \mathbf{D}^T(n+t)\, \mathbf{r}_{\mathrm{s}}(n)\, \mathbf{r}_{\mathrm{s}}{}^T(n+t)\, r_x(t) \left( \prod_{l=n+1+t}^{n-1} \mathbf{\Delta}(l) \right)^T. \end{aligned} \quad \text{(B.5)}$$

---

$$\begin{aligned} \tilde{\mathbf{f}}(n) &= \mathbf{\Delta}(n) \left[ \mathbf{\Delta}(n-1)\, \tilde{\mathbf{f}}(n-2) + \mathbf{D}(n-1)\, \mathbf{r}_{\mathrm{s}}(n-1)\, x(n-1) - \breve{\mathbf{f}}(n-1) \right] \\ &\quad + \mathbf{D}(n)\, \mathbf{r}_{\mathrm{s}}(n)\, x(n) - \breve{\mathbf{f}}(n) \\ &= \mathbf{\Delta}(n) \left[ \mathbf{\Delta}(n-1) \left\{ \mathbf{\Delta}(n-2)\, \tilde{\mathbf{f}}(n-3) + \mathbf{D}(n-2)\, \mathbf{r}_{\mathrm{s}}(n-2)\, x(n-2) - \breve{\mathbf{f}}(n-2) \right\} \right. \\ &\quad \left. + \mathbf{D}(n-1)\, \mathbf{r}_{\mathrm{s}}(n-1)\, x(n-1) - \breve{\mathbf{f}}(n-1) \right] + \mathbf{D}(n)\, \mathbf{r}_{\mathrm{s}}(n)\, x(n) - \breve{\mathbf{f}}(n) \ldots \\ &= \mathbf{\Delta}(n)\, \mathbf{\Delta}(n-1)\, \mathbf{\Delta}(n-2)\, \tilde{\mathbf{f}}(n-3) \\ &\quad + \mathbf{\Delta}(n)\, \mathbf{\Delta}(n-1) \left[ \mathbf{D}(n-2)\, \mathbf{r}_{\mathrm{s}}(n-2)\, x(n-2) - \breve{\mathbf{f}}(n-2) \right] \\ &\quad + \mathbf{\Delta}(n) \left[ \mathbf{D}(n-1)\, \mathbf{r}_{\mathrm{s}}(n-1)\, x(n-1) - \breve{\mathbf{f}}(n-1) \right] + \mathbf{D}(n)\, \mathbf{r}_{\mathrm{s}}(n)\, x(n) - \breve{\mathbf{f}}(n) \ldots \end{aligned} \quad \text{(B.2)}$$

In the above equation, the term $\left(\prod_{l=n+1+t}^{n-1} \mathbf{\Delta}(l)\right)$ can be simplified for $t = -t_0$, where the factors of $\mathbf{\Delta}(l)$ can be expressed following (A.12) as

$$\prod_{l=n-t_0+1}^{n-1} \mathbf{\Delta}(l) = \prod_{l=n-t_0+1}^{n-1} \left(\mathbf{I} - \mathbf{D}(n)\,\mathbf{r}_{\mathrm{s}}(n)\,\mathbf{q}^T(n) - \mathbf{D}(n)\,\mathbf{r}_{\mathrm{s}}(n)\,\mathbf{r}_{\mathrm{s}}^T(n)\right). \tag{B.6}$$

Expanding (B.6), collecting terms and substituting into (B.5), it can be observed that apart from $\mathbf{I}$, all other terms result in higher-order terms consisting of $\mathbf{D}(n)\,\mathbf{D}^T(n+t)\,\mathbf{r}_{\mathrm{s}}(n)\,\mathbf{r}_{\mathrm{s}}{}^T(n+t)$ in (B.5) and can be neglected. Hence, we can rewrite (B.6) as

$$\prod_{l=n-t_0+1}^{n-1} \mathbf{\Delta}(l) \approx \mathbf{I}. \tag{B.7}$$

Substituting (B.7) into (B.5), we have

$$E\left[\mathbf{D}(n)\,\mathbf{r}_{\mathrm{s}}(n)\,x(n)\,\tilde{\mathbf{f}}^T(n-1)\right] = \sum_{t=-1}^{-t_0} \mathbf{D}(n)\,\mathbf{D}^T(n+t)\,\mathbf{r}_{\mathrm{s}}(n)\,\mathbf{r}_{\mathrm{s}}{}^T(n+t)\,r_x(t). \tag{B.8}$$

Here, it can be assumed that $\mathbf{D}(n)$ is varying slowly over time such that the variation in $\mathbf{D}(n)$ is slower than the decay of $r_x(t)$. Then, we have

$$\mathbf{D}(n)\,\mathbf{D}^T(n+t) = \mathbf{D}(n)\,\mathbf{D}^T(n). \tag{B.9}$$

Then, (B.8) can be expressed with the help of (B.9) as

$$E\left[\mathbf{D}(n)\,\mathbf{r}_{\mathrm{s}}(n)\,x(n)\,\tilde{\mathbf{f}}^T(n-1)\right] = \mathbf{D}(n)\,\mathbf{D}^T(n)\sum_{t=-1}^{-t_0} \mathbf{R}_{\mathrm{p}}(t)\,r_x(t), \tag{B.10}$$

where $\mathbf{R}_{\mathrm{p}}(t) = \mathbf{r}_{\mathrm{s}}(n)\,\mathbf{r}_{\mathrm{s}}{}^T(n+t)$ using the direct-averaging method.

*Evaluation of the term* $E\left[\tilde{\mathbf{f}}(n-1)\,x(n)\,\mathbf{r}_s{}^T(n)\,\mathbf{D}(n)\right]$

Substituting (B.3) into (A.16) similarly as above for the term $E\left[\tilde{\mathbf{f}}(n-1)\,x(n)\,\mathbf{r}_{\mathrm{s}}{}^T(n)\,\mathbf{D}(n)\right]$, we have

$$E\left[\tilde{\mathbf{f}}(n-1)\,x(n)\,\mathbf{r}_{\mathrm{s}}^T(n)\,\mathbf{D}(n)\right] = \mathbf{D}(n)\,\mathbf{D}^T(n)\sum_{t=1}^{t_0} \mathbf{R}_{\mathrm{p}}(t)\,r_x(t). \tag{B.11}$$

Substituting (B.10) and (B.11) into (A.16), we get the final expression for $\bar{\mathbf{F}}_{\mathrm{a}}(n)$ in (A.17).

*Evaluation of diagonal elements of* $\frac{1}{L_f}\mathbf{\Gamma}\,\mathbf{D}(n)\,\mathbf{\Gamma}^H$

To obtain the expression for $\hat{\zeta}(\omega, n)$, the time-average shaped probe noise signal correlation matrix $\mathbf{R}(n)$ for the RLS algorithm in Fig. 2 can be expressed after the addition of the regularization term in the cost function as

$$\mathbf{R}(n) = \sum_{i=1}^{n} \lambda^{n-i} \mathbf{r}_{\mathrm{s}}(i)\, \mathbf{r}_{\mathrm{s}}^{T}(i) + \delta\, \lambda^{n}\, \mathbf{I} \tag{B.12}$$

where $\mathbf{R}(n)$ is a diagonal matrix and $\mathbf{I}$ is the $L_f \times L_f$ identity matrix [11]. Asymptotically, for a large value of $n$ and as $\lambda to 1$, the matrix $\sum_{i=1}^{n} \lambda^{n-i} \mathbf{r}_{\mathrm{s}}(i)\, \mathbf{r}_{\mathrm{s}}^{T}(i)$ tends to have large values [14]. As a result, $\mathbf{R}^{-1}(n)$ tends to contain small entries and $\mathbf{D}(n)$ in (A.6) can be expressed as

$$\mathbf{D}(n) \approx \mathbf{R}^{-1}(n). \tag{B.13}$$

In (B.13), it is assumed that $\mathbf{R}^{-1}(n)$ has converged[2] such that $\mathbf{R}^{-1}(n) = \mathbf{R}^{-1}(n-1)$. Thus, $\mathbf{R}^{-1}(n)$ can be written by substituting (B.13) into (A.8) as

$$\mathbf{D}(n) \approx \lambda^{-1}\left[\mathbf{D}(n) - \mathbf{D}(n)\, \mathbf{r}_{\mathrm{s}}(n)\, \mathbf{r}_{\mathrm{s}}^{T}(n)\, \mathbf{D}(n)\right]. \tag{B.14}$$

Upon convergence, $\mathbf{D}(n)$ in (B.14) becomes a Toeplitz matrix. Following (A.18), $\mathbf{D}(n)$ can also be diagonalized as $\frac{1}{L_f}\mathbf{\Gamma}\,\mathbf{D}(n)\,\mathbf{\Gamma}^H$. Then, the diagonal entries of $\frac{1}{L_f}\mathbf{\Gamma}\;\mathbf{D}(n)\;\mathbf{\Gamma}^H$ can be written as

$$d(\omega, n) \approx \lambda^{-1}\Big(d(\omega, n) - d^2(\omega, n)\; S_{\mathrm{p}}(\omega)\Big). \tag{B.15}$$

The solution to the second-order difference equation of (B.15) can be written as (A.22).

[2]It is not necessarily implied that $n \to \infty$ for $\mathbf{R}^{-1}(n-1)$ to converge.

## Appendix C.

*Proof of Lemma 1*

*Proof.* The PTF expression in (16) is a first-order difference equation in terms of $\hat{\zeta}(\omega, n)$ and it can be expressed as

$$\eta(k) = \frac{\beta}{1 - \alpha\, k^{-1}} \tag{C.1}$$

where $\alpha, \beta$ are real numbers. The coefficient $\alpha$ determines the convergence rate of the feedback canceller and can be written in terms of the forgetting factor as[3]

$$\alpha = 2\lambda - 1, \tag{C.2}$$

whereas the coefficient $\beta$ in (C.1) can be expressed as

$$\beta = L_{\mathrm{f}} \frac{(1-\lambda)^2}{S_{\mathrm{p}}(\omega)} S_{x}(\omega) + S_{\bar{f}}(\omega). \tag{C.3}$$

As defined in (17), the convergence rate in this case is determined as the decay of $\hat{\zeta}(\omega, n)$, and can be computed in dB per iterative instant $n$ as

$$\mathrm{CR} = \frac{d}{dn} 10 \log_{10}\left(\beta |\alpha|^n\right), \tag{C.4}$$

where $\beta|\alpha|^n$ is the impulse response function of $\eta(k)$. Further solving (C.4), we have

$$\begin{aligned} \mathrm{CR} &= 10 \frac{d}{dn} \left( \frac{\ln(\alpha)^n}{\ln 10} \right) = 10 \left( \frac{\ln \alpha}{\ln 10} \right) \frac{d}{dn}(n) \\ &= 10 \log_{10}(\alpha). \end{aligned} \tag{C.5}$$

Substituting (C.2) in (C.5), we have

$$\mathrm{CR} = 10 \log_{10}(2\lambda - 1). \tag{C.6}$$

[3] In (C.2), we consider values of $\lambda$ such that $\lambda \to 1$. This allows for slow convergence of the RLS algorithm due to which a good approximation of $\bar{\mathbf{F}}(n)$ by $\bar{\mathbf{F}}_{\mathrm{a}}(n)$ can be obtained in (A.17).

It can be observed from the above equation that the convergence rate is neither dependent on the frequency nor on the incoming acoustic signal $x(n)$, but only dependent on $\lambda$. In fact, it decreases with increasing $\lambda$ and the convergence becomes slower. From (C.1), it can be seen that $\eta(k)$ is stable when the poles lie inside the unit circle, i.e. $|\alpha| < 1$. Thus, it can be said that the linear prediction-based feedback cancellation system with shaped probe noise (see Fig. 1) is stable for

$$0 < \lambda < 1. \tag{C.7}$$

Using (18), the steady-state behaviour of the aforementioned system can be expressed as

$$\hat{\zeta}(\omega, \infty) = \lim_{n \to \infty} \hat{\zeta}(\omega, n). \tag{C.8}$$

Substituting (16) into (C.8), we get

$$\begin{aligned} \hat{\zeta}(\omega, \infty) &= L_f \frac{1-\lambda}{2\, S_{\mathrm{p}}(\omega)} S_x(\omega) + \frac{S_{\breve{f}}(\omega)}{2(1-\lambda)} \\ &= L_f \frac{1-\lambda}{2\,|A(\omega)|^2 S_r(\omega)} S_x(\omega) + \frac{S_{\breve{f}}(\omega)}{2(1-\lambda)}. \end{aligned} \tag{C.9}$$

In the above equation, the first term denotes the steady-state error, i.e. the minimum possible value of $\hat{\zeta}(\omega, n)$ in the steady state, and the second term denotes the tracking error due to changes in the feedback path. It can be observed in (C.9) that $L_f$ and $S_x(\omega)$ are directly proportional to the steady-state error, while the steady-state error decreases with increase in $\lambda$ and $S_{\mathrm{p}}(\omega)$. The tracking error is independent of $S_{\mathrm{p}}(\omega)$ but its value increases with increase in the value of $\lambda$ for the feedback path variations when $S_{\breve{f}}(\omega) > 0$. This implies a slower tracking. Infact, the convergence rate in (C.6) is also independent of $S_{\mathrm{p}}(\omega)$, but dependent on $\lambda$. Hence, it can be said that the value of $\hat{\zeta}(\omega, \infty)$ in (C.9) is a trade-off between the steady-state behaviour for a time-invariant feedback path and the tracking ability for a time-varying feedback path. □

*Proof of Corollary 1*

*Proof.* Using (C.6), a required rate of convergence can be obtained by choosing the value of $\lambda$ as (20), where the convergence rate is in dB per iterative instant

$n$. For a time-invariant feedback path, ignoring the tracking error in (C.9) and rearranging the terms, we have the expression in (21) that can be used to select a value of $\lambda$ for obtaining a required steady-state error. □

## Appendix D.

*Proof of Corollary 2*

*Proof.* Consider the AFC system of Fig. 1. The weight update equation for NLMS algorithm is given as [11]

$$\hat{\mathbf{f}}\,(n) = \hat{\mathbf{f}}\,(n-1) + \mu\,(n)\,\mathbf{r}_{\mathrm{s}}\,(n)\,e\,(n)\,, \tag{D.1}$$

where $e\,(n)$ is expressed as (A.2) and $\mu\,(n)$ is written as

$$\mu\,(n) = \frac{\tilde{\mu}\,(n)}{\delta + \mathbf{r}_{\mathrm{s}}{}^{T}\,(n)\,\mathbf{r}_{\mathrm{s}}\,(n)}, \tag{D.2}$$

where $\tilde{\mu}\,(n)$ is the normalized step size parameter and $\delta$ is a positive real number. The term $\mathbf{r}_{\mathrm{s}}{}^{T}\,(n)\,\mathbf{r}_{\mathrm{s}}\,(n)$ in (D.2) can be expressed as

$$\mathbf{r}_{\mathrm{s}}{}^{T}\,(n)\,\mathbf{r}_{\mathrm{s}}\,(n) = L_f\,\hat{\sigma}^2_{\mathrm{p}}, \tag{D.3}$$

where $\hat{\sigma}^2_{\mathrm{p}}$ is an estimate of the shaped probe noise signal variance $\hat{\sigma}^2_{\mathrm{p}}$. However for $\tilde{\mu}\,(n) \to 0$, $\hat{\sigma}^2_{\mathrm{p}}$ can be replaced by $\sigma^2_{\mathrm{p}}$ in (D.3) [17]. This is because, for a small value of step size, the NLMS algorithm can have a low-pass influence on the loudspeaker signal [11]. Thus, we can rewrite (D.2) as

$$\mu\,(n) = \frac{\tilde{\mu}\,(n)}{\delta + L_f\;\sigma^2_{\mathrm{p}}}, \tag{D.4}$$

where $\sigma^2_{\mathrm{p}}$ is the variance of $r_{\mathrm{s}}\,(n)$. Following the proof of Theorem 1, the expression for approximated feedback estimation-error covariance matrix can be written as

$$\begin{aligned}\bar{\mathbf{F}}_{\mathrm{a}}\,(n) = \bar{\mathbf{F}}_{\mathrm{a}}\,(n-1) - \mu\,(n)\,\mathbf{R}_{\mathrm{p}}\,(0)\,\bar{\mathbf{F}}_{\mathrm{a}}\,(n-1) - \mu\,(n)\,\bar{\mathbf{F}}_{\mathrm{a}}\,(n-1)\,\mathbf{R}_{\mathrm{p}}\,(0) + \breve{\mathbf{F}}\,(n)\\ + \mu^2\,(n)\sum_{t=-t_0}^{t_0}\mathbf{R}_{\mathrm{p}}\,(t)\,r_x\,(t).\end{aligned} \tag{D.5}$$

Diagonalizing $\bar{\mathbf{F}}_{\mathrm{a}}(n)$ in (D.5) using DFT matrix $\mathbf{\Gamma}$, we have

$$\hat{\boldsymbol{\chi}}(n) = \mathbf{\Gamma}\,\bar{\mathbf{F}}_{\mathrm{a}}(n-1)\,\mathbf{\Gamma}^{H} + \mathbf{\Gamma}\,\breve{\mathbf{F}}(n)\,\mathbf{\Gamma}^{H} - \mu(n)\,\frac{1}{L_f}\mathbf{\Gamma}\,\mathbf{R}_{\mathrm{p}}(0)\,\mathbf{\Gamma}^{H}\,\mathbf{\Gamma}\,\bar{\mathbf{F}}_{\mathrm{a}}(n-1)\,\mathbf{\Gamma}^{H} - \mu(n)\,\frac{1}{L_f}\mathbf{\Gamma}\,\bar{\mathbf{F}}_{\mathrm{a}}(n-1)\,\mathbf{\Gamma}^{H}\,\mathbf{\Gamma}\,\mathbf{R}_{\mathrm{p}}(0)\,\mathbf{\Gamma}^{H} + \mu^{2}(n)\sum_{t=-t_0}^{t_0}\mathbf{\Gamma}\,\mathbf{R}_{\mathrm{p}}(t)\,\mathbf{\Gamma}^{H} r_x(t). \tag{D.6}$$

The diagonal elements of $\hat{\boldsymbol{\chi}}(n)$ are defined as the PTF approximation as

$$\hat{\zeta}(\omega,n) = (1-2\mu(n)\,S_{\mathrm{p}}(\omega))\,\hat{\zeta}(\omega,n-1) + L_f\;\mu^{2}(n)\;S_{\mathrm{p}}(\omega)\,S_x(\omega) + S_{\breve{f}}(\omega). \tag{D.7}$$

Substituting (D.4) into (D.7), we have the approximate PTF expression for the NLMS adaptive algorithm-based feedback cancellation system with shaped probe noise as (22). □

*Proof of Lemma 2*

*Proof.* Equation (22) is a first-order difference equation in $\hat{\zeta}(\omega,n)$ and can be written following (C.1), where $\alpha$ is frequency dependent as

$$\begin{aligned}\alpha &= 1 - 2\frac{\tilde{\mu}(n)}{\delta + L_f\,\sigma_{\mathrm{p}}^{2}}S_{\mathrm{p}}(\omega)\\ &= 1 - 2\frac{\tilde{\mu}(n)}{\delta + L_f\,\sigma_{\mathrm{p}}^{2}}|A(\omega)|^{2}S_r(\omega),\end{aligned} \tag{D.8}$$

whereas $\beta$ can be written as

$$\beta = L_f\frac{\tilde{\mu}^{2}(n)}{\left(\delta + L_f\,\sigma_{\mathrm{p}}^{2}\right)^{2}}S_{\mathrm{p}}(\omega)\,S_x(\omega) + S_{\breve{f}}(\omega) \tag{D.9}$$

From (C.1), it can be seen that the system is stable $|\alpha| < 1$ and therefore, the range of $\tilde{\mu}(n)$ which ensures stability of the system can be given as

$$0 < \tilde{\mu}(n) < \frac{\delta + L_f\,\sigma_{\mathrm{p}}^{2}}{\max_{\omega} S_{\mathrm{p}}(\omega)}. \tag{D.10}$$

We can express the steady-state behaviour of the system in Fig. 1 for the NLMS algorithm by substituting (22) into (C.8) as

$$\begin{aligned}\hat{\zeta}(\omega,\infty) &= \lim_{n\to\infty} L_f \frac{\tilde{\mu}(n)}{2\left(\delta + L_f\,\sigma_{\mathrm{p}}^2\right)} S_x(\omega) + \lim_{n\to\infty}\left(\delta + L_f\,\sigma_{\mathrm{p}}^2\right)\frac{S_{\breve{f}}(\omega)}{2\tilde{\mu}(n)\,S_{\mathrm{p}}(\omega)} \\ &= \lim_{n\to\infty} L_f \frac{\tilde{\mu}(n)}{2\left(\delta + L_f\,\sigma_{\mathrm{p}}^2\right)} S_x(\omega) + \lim_{n\to\infty}\left(\delta + L_f\,\sigma_{\mathrm{p}}^2\right)\frac{S_{\breve{f}}(\omega)}{2\tilde{\mu}(n)\,|A(\omega)|^2 S_r(\omega)}.\end{aligned} \tag{D.11}$$

In the above equation, the first term denotes the steady-state error and the second term denotes the tracking error due to changes in the feedback path. It can be seen from (D.11) that $L_f$ and $\tilde{\mu}(n)$ are directly proportional to the steady-state error, while the steady-state error decreases with increasing $\sigma_{\mathrm{p}}^2$. The tracking error is inversely proportional to the ratio $S_{\mathrm{p}}(\omega)/\left(\delta + L_f\,\sigma_{\mathrm{p}}^2\right)$, but increases with increasing $L_f$. It can be seen from (C.5) and (D.8) that the rate of convergence is dependent upon the ratio $S_{\mathrm{p}}(\omega)/\left(\delta + L_f\,\sigma_{\mathrm{p}}^2\right)$ and also decreases with increasing $L_f$. Also, the rate of convergence decreases and the tracking error increases owing to a small value of $|A(\omega)|^2$. □

*Proof of Corollary 3*

*Proof.* Substituting (D.8) into (C.5) and rearranging, a required given rate of convergence can be obtained for the step size $\tilde{\mu}(n)$ as (23). Similarly from (D.11), ignoring the tracking-error term and rearranging, the expression for determining the value of $\tilde{\mu}(n)$ to achieve a required value of $\hat{\zeta}(\omega,\infty)$ is obtained as (24). □

## Appendix E.

*Proof of Corollary 4*

*Proof.* The microphone signal in (5) can be rewritten as

$$y(n) = x(n) + F(k, n-1)\,q(n). \tag{E.1}$$

We can rewrite the expression for $e(n)$ in (6) as

$$\begin{aligned} e(n) &= x(n) - \Big(\hat{F}(k, n-1) - F(k, n-1)\Big) q(n) \\ &= x(n) - \tilde{F}(k, n-1)\, q(n). \end{aligned} \tag{E.2}$$

The RLS adaptive weight update equation for the feedback path estimation filter $\hat{F}(k)$ is given as [11]

$$\hat{\mathbf{f}}(n) = \hat{\mathbf{f}}(n-1) + \mathbf{D}(n)\,\mathbf{q}(n)\,e(n), \tag{E.3}$$

where

$$\mathbf{D}(n) = \frac{\mathbf{R}^{-1}(n-1)}{\lambda + \mathbf{q}^T(n)\,\mathbf{R}^{-1}(n-1)\,\mathbf{q}(n)} \tag{E.4}$$

and

$$\mathbf{R}^{-1}(n) \;=\; \lambda^{-1}\big[\mathbf{R}^{-1}(n-1) \;-\; \mathbf{D}(n)\,\mathbf{q}(n)\,\mathbf{q}^T(n)\,\mathbf{R}^{-1}(n-1)\big]. \tag{E.5}$$

The approximate feedback estimation-error covariance matrix can be written as

$$\begin{aligned} \bar{\mathbf{F}}_{\mathrm{a}}(n) = \bar{\mathbf{F}}_{\mathrm{a}}(n-1) &- \mathbf{D}(n)\,\mathbf{R}_q(0)\,\bar{\mathbf{F}}_{\mathrm{a}}(n-1) - \bar{\mathbf{F}}_{\mathrm{a}}(n-1)\,\mathbf{R}_q(0)\,\mathbf{D}(n) + \breve{\mathbf{F}}(n) \\ &+ \mathbf{D}(n)\,\mathbf{R}_q(0)\,r_x(0)\,\mathbf{D}(n) + E\Big[\mathbf{D}(n)\,\mathbf{q}(n)\,x(n)\,\tilde{\mathbf{f}}^T(n-1)\Big] \\ &+ E\Big[\tilde{\mathbf{f}}(n-1)\,x(n)\,\mathbf{q}^T(n)\,\mathbf{D}(n)\Big], \end{aligned} \tag{E.6}$$

where

$$\mathbf{R}_q(m) = \lim_{N\to\infty} \frac{1}{N} \sum_{n=1}^{N} \mathbf{q}(n)\,\mathbf{q}^T(n-m), \tag{E.7}$$

where $m$ is the time delay, using direct-averaging method. After further evaluating the terms $E\Big[\mathbf{D}(n)\,\mathbf{q}(n)\,x(n)\,\tilde{\mathbf{f}}^T(n-1)\Big]$ and $E\Big[\tilde{\mathbf{f}}(n-1)\,x(n)\,\mathbf{q}^T(n)\,\mathbf{D}(n)\Big]$ in (E.6) following Appendix B to obtain the final expression for $\bar{\mathbf{F}}_{\mathrm{a}}(n)$, we get

$$\begin{aligned} \bar{\mathbf{F}}_{\mathrm{a}}(n) = \bar{\mathbf{F}}_{\mathrm{a}}(n-1) &- \mathbf{D}(n)\,\mathbf{R}_q(0)\,\bar{\mathbf{F}}_{\mathrm{a}}(n-1) - \bar{\mathbf{F}}_{\mathrm{a}}(n-1)\,\mathbf{R}_q(0)\,\mathbf{D}(n) + \breve{\mathbf{F}}(n) \\ &+ \mathbf{D}(n)\,\mathbf{D}^T(n) \sum_{t=-t_0}^{t_0} \mathbf{R}_q(t)\,r_x(t). \end{aligned} \tag{E.8}$$

Following the proof of Theorem 1, we can diagonalize (E.8) using an $L_f \times L_f$ DFT matrix $\mathbf{\Gamma}$, which consists of complex entries, as

$$\hat{\zeta}(\omega, n) = \Big(1 - 2\,d(\omega, n)\,S_q(\omega)\Big)\hat{\zeta}(\omega, n-1) + L_f\,d^2(\omega, n)\;S_q(\omega)\,S_x(\omega) + S_{\breve{f}}(\omega), \tag{E.9}$$

where $d(\omega, n)$ is the diagonal entry of $\frac{1}{L_f}\mathbf{\Gamma}\,\mathbf{D}(n)\,\mathbf{\Gamma}^H$ and is expressed as

$$d(\omega, n) = \frac{1-\lambda}{S_q(\omega)} \tag{E.10}$$

and $S_x(\omega)$ is the PSD of the incoming desired acoustic signal $x(n)$ and is defined as the Fourier transform of $r_x(t)$. Then, the PTF of (15) for the linear prediction-based feedback cancellation design without probe noise (shown in Fig. 2) can be written as (28). □

*Proof of Lemma 3*

*Proof.* Following the proof of Lemma 1, the steady-state behaviour of the system in Fig. 2 can be expressed using (28) as

$$\hat{\zeta}(\omega, \infty) = L_f \frac{1-\lambda}{2\,S_q(\omega)} S_x(\omega) + \frac{S_{\breve{f}}(\omega)}{2(1-\lambda)}. \tag{E.11}$$

The expression for $\hat{\zeta}(\omega, \infty)$ in (E.11) is the sum of two terms. The first term denotes the minimum possible value of $\hat{\zeta}(\omega, n)$ in the steady state and the second term denotes the tracking error due to changes in the feedback path. In (E.11), it is seen that $L_f$ and $S_x(\omega)$ are directly proportional to the steady-state error, while the steady-state error decreases with increase in $S_q(\omega)$ and $\lambda$. The tracking error is unaffected by $S_q(\omega)$, but increases with increasing $\lambda$ for the feedback path variations when $S_{\breve{f}}(\omega) > 0$ leading to a slower tracking. Following the proof of Lemma 1, it can be concluded that the convergence rate is also unaffected by $S_q(\omega)$ , but depends on the value of $\lambda$ as shown in (C.6). So, it can be said that the overall value of $\hat{\zeta}(\omega, \infty)$ is a trade-off between the steady-state behaviour for a time-invariant feedback path and tracking behaviour for a time-varying feedback path. □

*Proof of Corollary 5*

*Proof.* The expression for selecting a forgetting factor value for RLS adaptive algorithm to obtain a required given rate of convergence for the AFC system without probe noise can be obtained following Corollary 1. Also, following Corollary 1 in ignoring the tracking-error term in (E.11) and rearranging, we

obtain the expression for choosing the value of $\lambda$ to obtain a desired steady-state error $\hat{\zeta}(\omega,\infty)$ as (29). □

## Appendix F.

*Proof of Corollary 6*

*Proof.* The weight update equation for the NLMS algorithm-based adaptive filter in Fig. 2 is given by [11]

$$\hat{\mathbf{f}}(n)=\hat{\mathbf{f}}(n-1)+\mu(n)\,\mathbf{q}(n)\,e(n), \tag{F.1}$$

where

$$\mu(n)=\frac{\tilde{\mu}(n)}{\delta+L_f\,\sigma_q^2}. \tag{F.2}$$

The expression for $\bar{\mathbf{F}}_{\mathrm{a}}(n)$ can be written as

$$\begin{aligned}\bar{\mathbf{F}}_{\mathrm{a}}(n)=\bar{\mathbf{F}}_{\mathrm{a}}(n-1)-\mu(n)\,\mathbf{R}_q(0)\,\bar{\mathbf{F}}_{\mathrm{a}}(n-1)-\mu(n)\,\bar{\mathbf{F}}_{\mathrm{a}}(n-1)\,\mathbf{R}_q(0)+\breve{\mathbf{F}}(n)\\+\mu^2(n)\sum_{t=-t_0}^{t_0}\mathbf{R}_q(t)\,r_{\boldsymbol{x}}(t).\end{aligned} \tag{F.3}$$

Diagonalizing $\bar{\mathbf{F}}_{\mathrm{a}}(n)$ in (F.3) using the DFT matrix $\boldsymbol{\Gamma}$, we have

$$\begin{aligned}\hat{\boldsymbol{\Psi}}(n)=\boldsymbol{\Gamma}\bar{\mathbf{F}}_{\mathrm{a}}(n-1)\,\boldsymbol{\Gamma}^H+\boldsymbol{\Gamma}\breve{\mathbf{F}}(n)\,\boldsymbol{\Gamma}^H-\mu(n)\,\frac{1}{L_f}\boldsymbol{\Gamma}\,\mathbf{R}_q(0)\,\boldsymbol{\Gamma}^H\,\boldsymbol{\Gamma}\,\bar{\mathbf{F}}_{\mathrm{a}}(n-1)\,\boldsymbol{\Gamma}^H\\-\mu(n)\,\frac{1}{L_f}\boldsymbol{\Gamma}\,\bar{\mathbf{F}}_{\mathrm{a}}(n-1)\,\boldsymbol{\Gamma}^H\,\boldsymbol{\Gamma}\,\mathbf{R}_q(0)\,\boldsymbol{\Gamma}^H+\mu^2(n)\sum_{t=-t_0}^{t_0}\boldsymbol{\Gamma}\,\mathbf{R}_q(t)\,\boldsymbol{\Gamma}^H r_x(t).\end{aligned} \tag{F.4}$$

The diagonal elements of $\hat{\boldsymbol{\Psi}}(n)$ are defined as the PTF of (15), and expressed as

$$\hat{\zeta}(\omega,n)=\Big(1-2\mu(n)\,S_q(\omega)\Big)\hat{\zeta}(\omega,n-1)+L_f\,\mu^2(n)\;S_q(\omega)\,S_x(\omega)+S_{\breve{f}}(\omega). \tag{F.5}$$

Substituting the expression for $\mu(n)$ from (F.2) into (F.5), we have the PTF of (15) for the NLMS adaptive-algorithm-based feedback cancellation system without probe noise as (30). □

*Proof of Lemma 4*

*Proof.* Following the proof of Lemma 2, we have from Corollary 6

$$\alpha = 1 - 2\frac{\tilde{\mu}\,(n)}{\delta + L_f\,\sigma_q^2} S_q\,(\omega)\,, \tag{F.6}$$

and

$$\beta = L_f\,\frac{\tilde{\mu}^2\,(n)}{\left(\delta + L_f\,\sigma_q^2\right)^2}\,S_q\,(\omega)\,S_x\,(\omega) + S_{\breve{f}}\,(\omega)\,. \tag{F.7}$$

The AFC system in Fig. 2 is stable for the range for $\tilde{\mu}\,(n)$ given as

$$0 < \tilde{\mu}\,(n) < \frac{\delta + L_f\,\hat{\sigma}_q^2}{\max_\omega S_q\,(\omega)}. \tag{F.8}$$

The steady-state behaviour of the feedback cancellation system in Fig. 2 can be expressed as

$$\hat{\zeta}\,(\omega,\infty) \;=\; \lim_{n\to\infty} L_f \frac{\tilde{\mu}\,(n)}{2\left(\delta + L_{\mathrm{f}}\,\sigma_q^2\right)} S_x\,(\omega) \;+\; \lim_{n\to\infty} \left(\delta + L_f\,\sigma_q^2\right) \frac{S_{\breve{f}}\,(\omega)}{2\tilde{\mu}\,(n)\,S_q\,(\omega)}. \tag{F.9}$$

The expression for $\hat{\zeta}\,(\omega,\infty)$ in (F.9) is the sum of two terms. The first term denotes the minimum possible value of $\hat{\zeta}\,(\omega,n)$ in the steady state and the second term denotes the tracking error due to changes in the feedback path. It can be seen from (F.9) that both $L_f$ and the step size $\tilde{\mu}\,(n)$ are directly proportional to the steady-state error, while the steady-state error decreases with increase in $\sigma_q^2$. Owing to the presence of $\sigma_q^2$, the tracking error is inversely proportional to the ratio $S_q\,(\omega)\,/\left(\delta + L_f\,\sigma_q^2\right)$ instead of only the value of $S_q\,(\omega)$. Also, the tracking error is increased with an increase in $L_f$. Similarly, it can be seen from (C.5) and (F.6) that the convergence rate is dependent upon the ratio $S_q\,(\omega)\,/\left(\delta + L_f\,\sigma_q^2\right)$ and decreases with increase in $L_f$. □

*Proof of Corollary 7*

*Proof.* Following the proof of Corollary 3, the expression for $\tilde{\mu}\,(n)$ for a given rate of convergence can be obtained from (F.9) as (31), where the convergence rate is in dB per iterative instant $n$. Similarly, using (F.9) and ignoring the tracking error, we have the expression for determining the value of $\tilde{\mu}\,(n)$ for obtaining a desired steady-state error $\hat{\zeta}\,(\omega,\infty)$ as (32). □